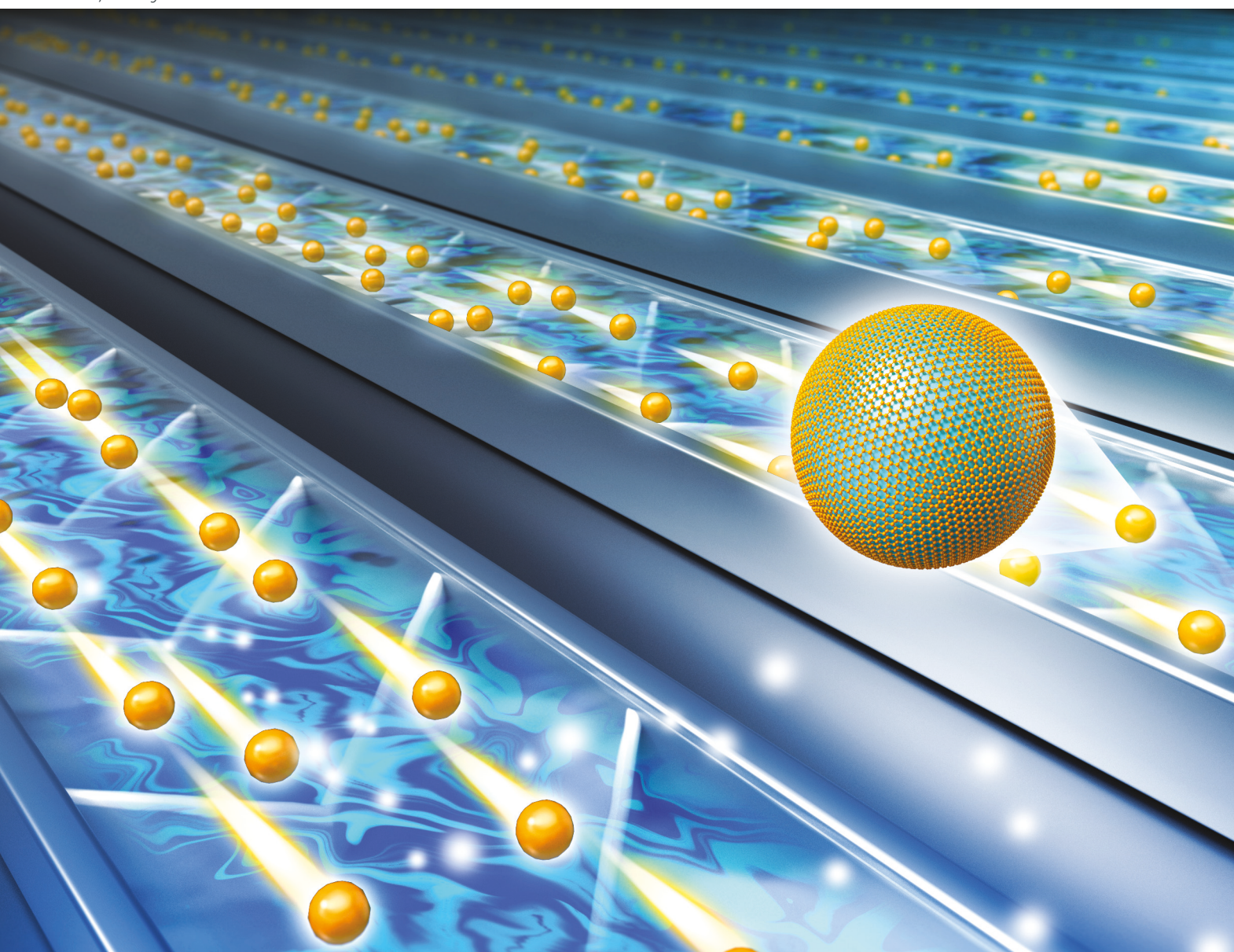
Volume 149 Number 3 7 February 2024 Pages 587-976

Analyst

rsc.li/analyst



ISSN 0003-2654



CRITICAL REVIEW

Yingnan Shen, Bumsoo Han *et al.* Advanced manufacturing of nanoparticle formulations of drugs and biologics using microfluidics



CRITICAL REVIEW

View Article Online
View Journal | View Issue



Cite this: Analyst, 2024, 149, 614

Advanced manufacturing of nanoparticle formulations of drugs and biologics using microfluidics

Yingnan Shen, (1) ** Hogyeong Gwak (1) and Bumsoo Han (1) **a,b

Numerous innovative nanoparticle formulations of drugs and biologics, named nano-formulations, have been developed in the last two decades. However, methods for their scaled-up production are still lagging, as the amount needed for large animal tests and clinical trials is typically orders of magnitude larger. This manufacturing challenge poses a critical barrier to successfully translating various nano-formulations. This review focuses on how microfluidics technology has become a powerful tool to overcome this challenge by synthesizing various nano-formulations with improved particle properties and product purity in large quantities. This microfluidic-based manufacturing is enabled by microfluidic mixing, which is capable of the precise and continuous control of the synthesis of nano-formulations. We further discuss the specific applications of hydrodynamic flow focusing, a staggered herringbone micromixer, a T-junction mixer, a micro-droplet generator, and a glass capillary on various types of nano-formulations of polymeric, lipid, inorganic, and nanocrystals. Various separation and purification microfluidic methods to enhance the product purity are reviewed, including acoustofluidics, hydrodynamics, and dielectrophoresis. We further discuss the challenges of microfluidics being used by broader research and industrial communities. We also provide future outlooks of its enormous potential as a decentralized approach for manufacturing nano-formulations.

Received 10th October 2023, Accepted 28th November 2023 DOI: 10.1039/d3an01739g rsc.li/analyst

1. Introduction

Numerous innovative nanoparticle formulations have been developed for targeted and improved drug delivery. 1-3 Early efforts focused on chemotherapeutic drugs for oncology applications. However, many of these formulations were developed and tested using preclinical small animal models. It is still challenging to translate these into large animal tests and clinical trials. For now, only twenty-eight nanoparticle therapeutics (including COVID-19 vaccines with emergency use authorization) have been approved for clinical use.4-7 A major hindrance lies in the dramatic increase of the amount of nanoparticles (NPs) needed for clinical trials compared to small animal tests. For example, antitumor nano-formulations may require hundreds of grams of NPs for a phase 1A clinical trial.^{8,9} Thus, scaling up for production is one of the technical gaps when researching and testing many nano-formulations in more clinically relevant settings.

Large-scale production is technically challenging as batchto-batch variations in the physiochemical properties may occur due to the polydispersity of NPs, which can induce inconsistencies in preclinical or clinical trials. 10,11 Conventional batch production methods or reactors include solvent evaporation for polymeric NPs, 12-14 extrusion for lipid nanoparticles (LNPs), 15,16 and a static mixer for nanocrystals. 17-19 These batch synthesis methods operate at the millimeter or even centimeter scale, resulting in a uniform mixing environment where local fluctuations of concentration occur and lead to the formation of NPs with large sizes and a wide size distribution. NP size and shape are crucial physicochemical properties to control during the synthesis process as they directly influence the therapeutic efficacy of NPs, such as in vivo biodistribution and retention ability in tissues, as well as take up and clearance by macrophages.20-22 Batch production methods may generate polymeric NPs with uncontrolled size and limited drug loading, resulting in short half-life of biodistribution, 4,23 or LNPs with a high polydispersity index (PDI), leading to limited tissue penetration;24,25 worse, nanocrystals produced by batch methods have a wide range of sizes, depending on the type of hydrophobic drugs. 26-28 Therefore, microfluidic platforms are developed and employed to scale up the manufacturing of nano-formulations. The utilization of microflui-

^aSchool of Mechanical Engineering, Purdue University, West Lafayette, IN 47907, USA. E-mail: shen453@purdue.edu, bumsoo@purdue.edu; Tel: +1-765-494-5626 ^bPurdue University Institute for Cancer Research, West Lafayette, IN, 47907, USA

dics not only avoids labor-intensive multistep processes for research labs, but also avoids batch-to-batch variations with its continuous manner of NP synthesis. Microfluidics also enables the precise control of the synthesis process, which leads to convenient modification of the physicochemical pro-

perties of NPs. Firstly, we explain how microfluidics can bring high consistency and reproducibility to nano-formulation synthesis by controlled rapid mixing of pico- to nanoliter volumes of fluids from the perspective of separating the NP formation stages of nucleation, growth, and aggregation. Then we specifically introduce the microfluidic mixing techniques of hydrodynamic flow focusing, a staggered herringbone micromixer, a T-junction mixer, a micro-droplet generator, and a glass capillary, as well as their applications in the synthesis of polymeric NPs, lipid NPs, inorganic NPs, and nanocrystals with improved physical properties and in vivo behavior. Microfluidic techniques to separate and purify nano-drugs and biologics are also summarized, including both the passive and active techniques of acoustofluidics, hydrodynamics, and dielectrophoresis. Finally, we discuss the current challenges of the utilization of microfluidics by broader research and industrial communities due to the high entry level and fabrication complexity. It has enormous potential as a decentralized approach for the manufacturing of NP-based drug formulations, ideally to

2. Mechanisms for the formation of drug nanoparticles using microfluidics

meet the specific needs of individuals.

The microfluidics techniques of hydrodynamic flow focusing, a staggered herringbone micromixer, a T-junction mixer, a micro-droplet generator, and a glass capillary lead to precise

control over nanoliter volumes of fluid in a device with microscale dimensions, and thus a short microfluidic mixing timescale on the order of milliseconds is achieved, which enables control of the nanoprecipitation-based NP formation process.²⁹ Specifically, the concurrent occurrence of the NP formation stages of nucleation, growth, and aggregation induces significant batch-to-batch variations in conventional batch methods.30,31 By comparison, microfluidic platforms, with their short mixing timescales, do a better job at separating the three NP stages. 32-36 The mixing timescale related mechanism to explain different NP formation dynamics induced by microfluidic mixing and batch mixing is illustrated in Fig. 1. The microfluidic mixing timescale $(\tau_{\rm m})$ can be tuned to be shorter than the drug's nucleation timescale (τ_n) , so the drug solute concentration quickly exceeds the saturation concentration (c_s) and reaches the critical nucleation concentration (c_n) , leading to the generation of evenly distributed precursors for nucleation (prenucleation drug molecule clusters). Then the concentration of drug solute quickly drops when homogeneous nucleation is initiated. Homogeneous nucleation dominates over particle growth to consume the remaining drug molecules or clusters, which enables the synthesis of small and uniform NPs. The batch mixing timescale (τ'_m) is longer than τ_n , which means that mixing is still not completed when nucleation starts. Nuclei are generated but there is still a large amount of solutes dissolved in the organic phase, so particle growth dominates over heterogeneous nucleation to consume the remaining drug molecules, resulting in NPs with larger size and higher PDI.

Precisely prepared microfluidic channels with dimensions of tens to hundreds of micrometers enable high levels of control over the fluids in the laminar flow regime. The microfluidic mixing mechanism is based on the interdiffusion of solvent molecules obtained by means of laminar flows. Hence,

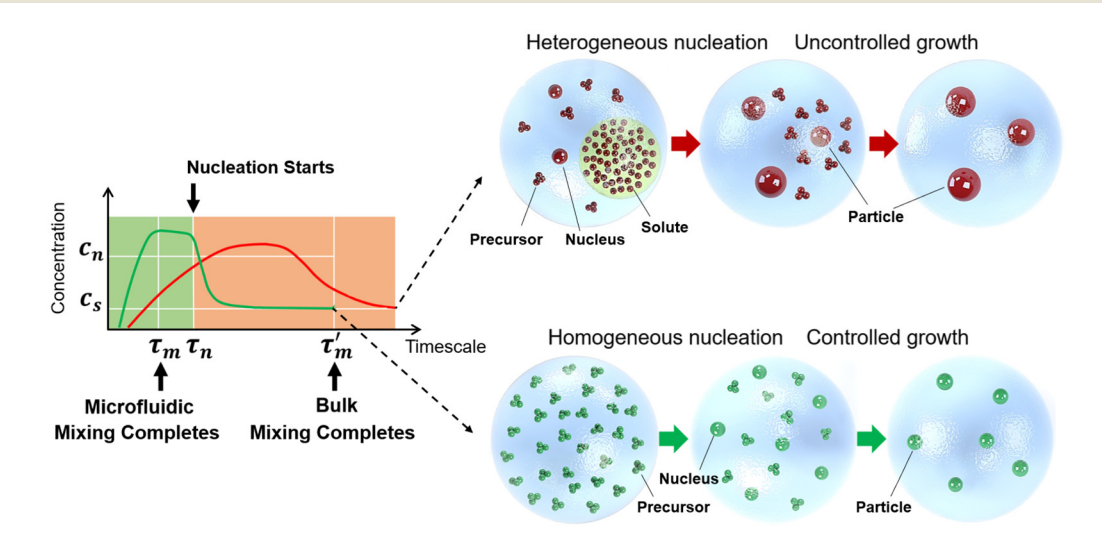


Fig. 1 Schematic explanation of the different NP formation dynamics induced by microfluidic mixing and batch mixing. The shorter microfluidic mixing timescale (τ_m) than the drug's nucleation timescale (τ_n) (i.e., green line) induces homogeneous nucleation and controlled growth of particles, while a longer mixing timescale (τ_m) than τ_n such as batch mixing (i.e., red line) leads to heterogeneous nucleation and uncontrolled growth of particles.

Critical Review Analyst

microfluidic mixing can be characterized by the Reynolds number, Re, and the Peclet number, Pe.

$$Re = \frac{\rho uL}{\mu} \tag{1}$$

where ρ and μ are the density and viscosity of the fluid, respectively, u is the flow speed, and L is the characteristic length of the channel. The Reynolds number is a dimensionless quantity characterizing flow patterns. The occurrence of turbulent flow is indicated when Re > 2000–4000. 37

$$Pe = \frac{uL}{D} \tag{2}$$

where D is the diffusivity. The Peclet number describes the relative importance of mass transport by diffusion (across the channel) and by convection (along the channel). In order to generate predictable mixing patterns, microfluidic mixing is mostly designed to operate at Re < 2000 to avoid turbulent flows, which have random streamlines. 31,38 Our previous work on the microfluidic synthesis of drug nanocrystals shows streamlined distribution in a microfluidic mixing device in the Reynolds number range of 5-250 where straight and parallel streamlines are present at Re = 5 while micro-vortices can occur at Re = 25 in the water-ethanol mixing region.³⁹ The constraint of the Reynolds number leads to an upper limit of the Peclet number of 250-2500.40 The precise control of mixing between fluids is not possible using conventional batch methods but can be achieved in microfluidics in a continuous manner with predictable mixing efficiency, which enables control over the NP formation processes of nucleation, growth, and aggregation, and thus the limitations on uniformity and consistency of NP characteristics can be overcome with microfluidic synthesis platforms.

Microfluidic platforms have been utilized to produce NPs with a smaller size, narrower size distribution (i.e. smaller PDI), and improved drug loading and encapsulation efficiency.²³ To achieve this, nanoprecipitation is induced in the microchannel via rapid mixing of solvent and anti-solvent. Several microfluidic mixing techniques have been developed without the involvement of external fields, including hydrodynamic flow focusing (HFF), a staggered herringbone micromixer (SHM), a T-junction mixer, a micro-droplet generator, and a glass capillary. These microfluidic mixing methods are employed to produce various types of NPs including polymeric NPs, LNPs, inorganic NPs, and drug nanocrystals. Low Reynolds numbers (generally less than 100)41 indicate steady state and fully developed laminar flow regimes during microfluidic mixing, and hence mass transfer can be considered to depend solely on diffusion. The mixing time ($\tau_{\rm m}$), which is a measure of the solvent exchange efficiency, quadratically depends on the diffusion length between solvents. $\tau_{\rm m}$ can be defined as

$$\tau_m = \frac{x^2}{2D} \tag{3}$$

where x is the diffusion length and D is the diffusion coefficient. Therefore, diffusion-based microfluidic mixing methods rely on reducing the diffusion length to control the mixing time to provide a homogeneous environment for NP formation.

HFF is a powerful tool to reduce the diffusion length between mixing solvents with stable control. As schematically shown in Fig. 2A, HFF is commonly a three-inlet microfluidic device that generates a central flow with side flows. The flow regime of HFF develops when fluids with different velocities are introduced into the mixing channel side by side. 43 The central fluid flows at a much lower velocity than the side fluid in the same channel. As a result, the central fluid (organic phase) containing the samples of interest is sheathed in a thin sheet of the side fluid (aqueous phase) to achieve fast mixing between the two fluids. Fig. 2B shows the schematic structure of the SHM. The microfluidic SHM has two inlets and utilizes repeated patterns of asymmetric protrusions to induce passive mixing by chaotic stirring, which greatly reduces the diffusion length between the two fluids. 44,45 Chaotic stirring can be induced by the asymmetric protrusions at low Reynolds numbers (Re < 100).46 Efficient mixing of the organic and aqueous fluids can be achieved within 10 or 15 cycles of the repeat patterns.47 Fig. 2C shows microfluidic droplet-based mixing, which confines the chemical reactions to picolitersized droplets. The droplet generators are commonly used for inorganic NP synthesis.48 Aqueous droplets containing the seeds of NPs and other reagents for the reaction are generated in the form of water-in-oil emulsions. In a T-junction mixer, two fluids flow directly toward each other with a perpendicular output. The simple T-junction mixer shown in Fig. 2D (left) is not able to reduce the diffusion length when it operates with stratified laminar flows.49 To enhance mixing, the T junction can be designed with dimensions in the millimeter range and operate under turbulent or transitional conditions (Re > 2000).50 To enable the T junction to work in the microfluidic mixing scenario (Re < 100), the vortex micro T-mixer has been developed to form vortex flows at low Reynolds numbers.^{51,52} Fig. 2D (right) shows the generation of vortex flows in the mixing channel by two fluids flowing through non-aligned inlets. Two-dimensional HFF (Fig. 2A) squeezes the central fluid horizontally but not vertically. Fig. 2E shows a microfluidic device enabling the three-dimensional (3D) squeezing of the central fluid with the generation of microvortices upstream of 3D flow focusing. 53,54 The benefit of 3D flow focusing lies in the elimination of the interface between the central fluid and the wall of the microchannel, which can significantly reduce NP attachment and minimize the risk of channel clogging. 55-57 Another approach for 3D flow focusing is the microfluidic device of a glass capillary (Fig. 2F). The glass capillary device is prepared by inserting tapered cylindrical capillaries into a square capillary.⁵⁸ Similar to 2D HFF, the organic solvent is the inner phase, and the aqueous solution is the outer phase. The inserted glass capillary positions the organic solvent at the center of the mixing channel in all directions. Thus, the organic-aqueous interface, where the NPs are predominantly

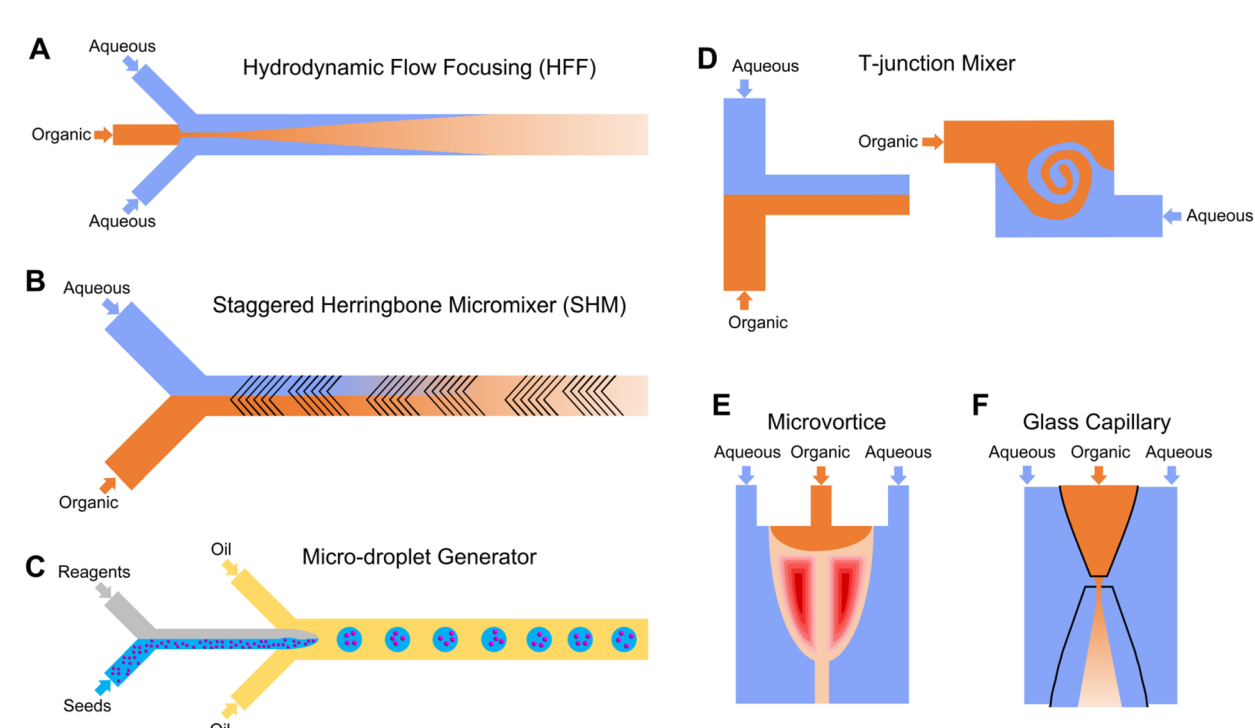


Fig. 2 Schematics of the microfluidic mixing techniques for the synthesis of nanomedicines. (A) Hydrodynamic flow focusing (HFF). (B) Staggered herringbone micromixer (SHM). (C) Micro-droplet generator. (D) T-junction mixer. (E) 3D flow focusing with microvortices. (F) Glass capillary.

formed, is fully displaced from the walls of the mixing channel. 59

To scale up the production of NPs at clinically or industrially relevant levels, three strategies can be adopted in microfluidic settings. First, the flow rate through the microchannel can be regulated according to the timescale-based mechanism discussed in Fig. 1. This strategy enables the determination of the optimal flow rate range to achieve high throughput synthesis of NPs while maintaining the quality of NPs including size and drug loading. As shown in Fig. 3A, our group proposed a timescale-based mechanism to optimize the HFF conditions for both synthesis quality and throughput. We noticed an increase in NP size and a decrease in drug loading when the flow rate was increased to 102.5 mL h⁻¹ due to the accumulation of organic solvent in the bifurcated streams. This issue could be resolved when the flow rate was further increased to 205 mL h⁻¹, while maintaining a good quality of NPs approximately 100 nm in size, 0.1 PDI, 70% encapsulation efficiency, as well as 50% drug loading.39 The second strategy to further increase throughput is to introduce strong convective mixing into the microchannel. However, a high inlet flow pressure is required, and high-pressure capacity of the tubing interconnection needs to be developed to avoid liquid leakage. As shown in Fig. 3B, a robust tubing method was developed to sustain a pressure of up to 4.5 MPa. This high-pressure tubing technique enables strong convective mixing at a high flow rate of 410 mL h⁻¹, resulting in the size-controlled synthesis of small PLGA NPs of 55 nm in diameter with good dispersion. The mass production of PLGA NPs can reach 200-800 mg h⁻¹.60

Combined with the first two strategies, the third strategy to scale up throughput is to arrange the microchannels in parallel. In Fig. 3C, a pressure-tolerant (up to 16 MPa) 3D-HFF device with eight parallel microchannels was used to prepare PLGA NPs. The NP size was reproducibly controlled between 50 and 150 nm at a flow rate up to 1440 mL h⁻¹, which enabled a mass production rate of approximately 1300 mg h⁻¹. These scale-up strategies show the potential for microfluidic synthesis to meet clinical or even industrial purposes.

3. Microfluidic synthesis and separation strategies for nanoformulations

Nano-formulations can encompass both organic and inorganic materials of synthetic or natural origin for nanomedicine, and hence can be classified as organic or inorganic NPs. 62 Inorganic NPs offer great opportunities in nanomedicine to serve as therapeutic or imaging agents. Commonly used materials for inorganic NPs include metals, metallic oxides, and semiconductors. 63 Organic NPs can be further divided into polymeric NPs, lipid NPs, and (small molecule) drug nanocrystals. Here we discuss microfluidic synthesis strategies for these different types of nano-formulations, as well as the microfluidic separation and purification of nano-drug and biologics.

Critical Review Analyst

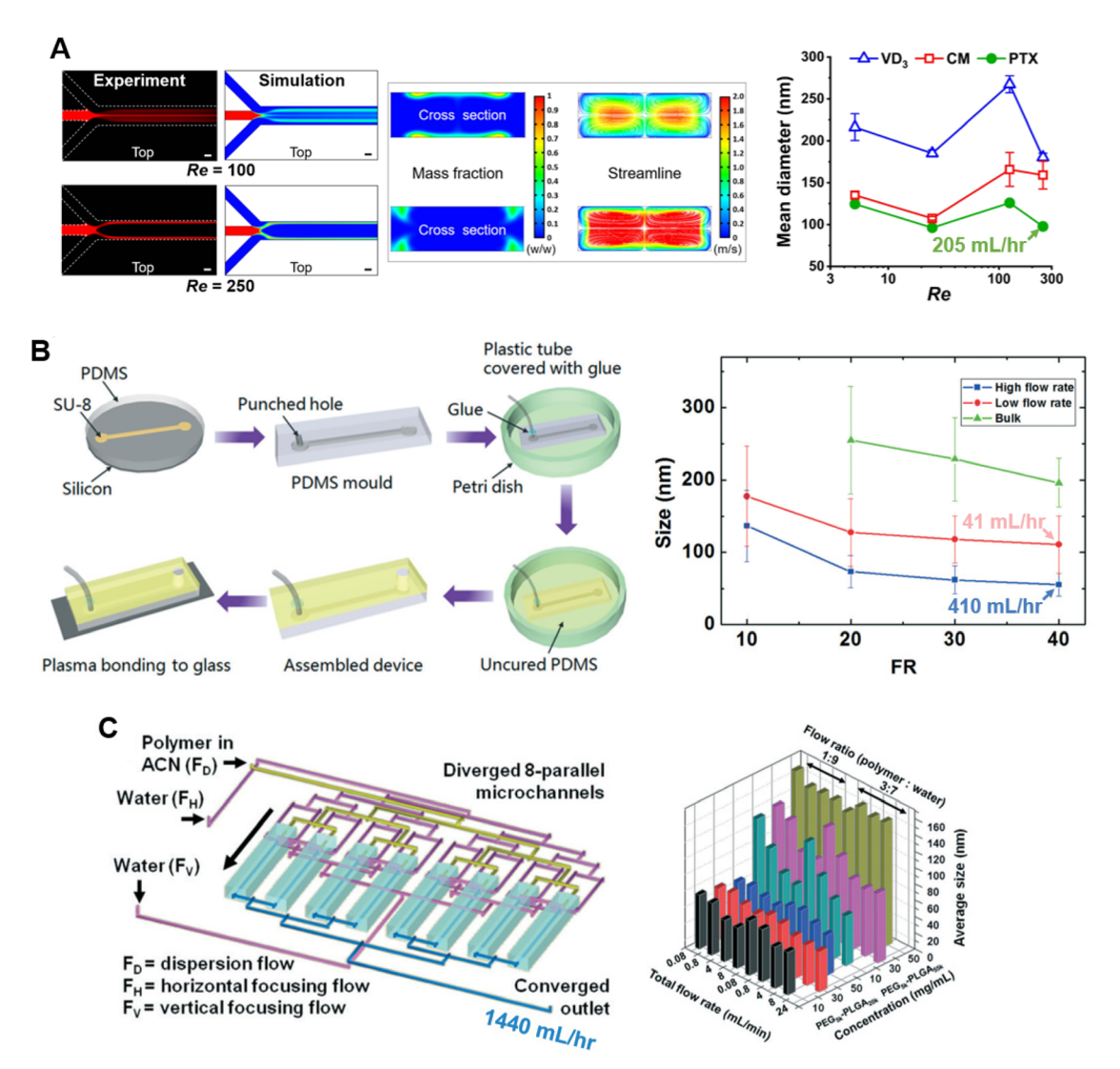


Fig. 3 Scale-up strategies for the microfluidic synthesis of NPs. (A) Timescale-based optimization of the flow rate conditions in a single microchannel. A flow rate of 205 mL h^{-1} was achieved to produce quality-controlled NPs of hydrophobic drugs with a size of approximately 100 nm. Reprinted with permission from ref. 39. Copyright 2023 Elsevier. (B) Enhanced convective mixing in a microchannel with pressure-tolerant designs. A flow rate of 410 mL h⁻¹ was achieved to produce PLGA NPs while maintaining their small size of 55 nm. Reprinted with permission from ref. 60. Copyright 2013 Royal Society of Chemistry. (C) Pressure-tolerant microfluidic device with multiple parallel microchannels. The total flow rate of eight microchannels reached 1440 mL h⁻¹, which enabled a mass production rate up to 1300 mg h⁻¹. Reprinted with permission from ref. 61. Copyright 2014 Royal Society of Chemistry.

3.1. Polymeric NPs

Polymeric NPs are one of the most studied formulations as nanomedicines with applications from drug delivery to imaging. Poly(lactic-co-glycolic acid) (PLGA) stands out as the most clinically advanced polymer for its hydrophobicity, which enables easy nanoprecipitation for NP formation and loading of hydrophobic drugs (such as paclitaxel) into PLGA NPs.64 PLGA also shows good biodegradability and biocompatibility with negligible effects on organisms in most cases. 65,66 Another good example is polyethylene glycol (PEG), which has become the most popular polymeric molecule for the coating of NPs. 67 PEG sterically stabilized the NPs by forming a hydro-

philic layer on the surface of NPs. 68 The controlled release properties of polymeric NPs rely on the controlling properties of polymers, which alter the release profiles of the encapsulated drugs.69 The conventional batch method of solvent evaporation involves multiple time-consuming steps for the production and post processing of emulsions; moreover, the batch produced polymeric NPs typically have big sizes of over 150 nm, limited drug loading, as well as significant batch-tobatch variations.

The microfluidic synthesis of polymeric NPs can be conducted in different devices of HFF, a SHM, a micro-droplet generator, and a glass capillary. HFF is the most commonly used microfluidic method in polymeric NP studies, where a

central stream of polymer-containing organic solvent is squeezed by the side aqueous streams flowing at a much higher speed. Fig. 4A shows details of a study to synthesize PLGA-PEG NPs by rapidly mixing polymer-acetonitrile solutions and water using the HFF device. 23 The PLGA-PEG NPs prepared by a batch mixing method increased dramatically in size with the addition of free PLGA to the precursor solution, but the size of NPs produced by the HFF method remained relatively unchanged with an increase of the PLGA concentration up to 50 mg mL⁻¹. Moreover, the half-life of the encapsulated drug docetaxel is longer in the microfluidic NPs than that in the batch NPs (19 h versus 11 h). Fig. 4B shows details of a study that proposed a variation of the design of the HFF device. 70 The HFF chips were manually folded to form the geometries of an arc and double spiral to facilitate mixing. The combination of HFF and 3D curved microchannels was found to significantly reduce the mixing time, which enabled the synthesis of doxorubicin (DOX)-loaded PLGA with good size control at higher throughput. The HFF-synthesized PLGA NPs were also found to significantly improve the stability of the encapsulated drug curcumin with a half-life of 2 days; in comparison, the half-life of the free drug curcumin was as short as 30 minutes.⁷¹ To avoid channel clogging by polymer aggregates, PDMS-based 3D HFF devices were developed to reduce the organic stream-channel wall interface and showed no

channel fouling after running the synthesis of PLGA-PEG NPs

for over 10 minutes.55

The study shown in Fig. 4C enabled the synthesis of polymeric NPs via droplet-based microfluidics. 72 The polymers hyaluronic acid (HA) and linear polyethyleneimine (LEPI) were covalently crosslinked in each droplet to produce highly monodisperse polymeric NPs with tunable sizes of 92-190 nm and a very small PDI of 0.015. The release of encapsulated DOX exhibited an enhanced antiblastic effect even at sublethal dosages, highlighting the applicability of this droplet-based microfluidic method in nanomedicine scenarios. The efficient production of PLGA NPs is also feasible using the SHM. The study illustrated in Fig. 4D optimized the total flow rate (TFR) and flow rate ratio (FRR) of the aqueous and organic solutions introduced into the SHM device for the synthesis of PLGA NPs tagged with cell-penetrating peptides (CPP). The distribution of the CPPs (Au-labeled) throughout the PLGA NPs was only observed when the PLGA NPs were prepared with a conjugation approach based on an in situ SHM.73 The example of the application of a glass capillary, as a variation of 3D HFF, for the synthesis of polymeric NPs is provided in Fig. 4E.58 The curcumin-loaded shellac NPs were produced by injecting the ethanolic polymer solution from the tapered cylindrical capillary into the water-containing outer square capillary. The mixing time was estimated at 9 ms with a mixing length of 1.6 mm when the glass capillary device was operating under the parameters of TFR = 20 mL h^{-1} and FRR = 40. A highencapsulation efficiency of 98% for curcumin was achieved indicating that the glass capillary synthesis method could be robust and reproducible for the encapsulation of hydrophobic drugs in biocompatible polymeric NPs. Not only encapsulation

efficiency, but also release kinetics and the anticancer effect of the polymeric NPs can be improved when prepared using microfluidic methods. For example, one study encapsulated gemcitabine in PLGA NPs using the microfluidic mixing device of HFF. Tompared to the gemcitabine-loaded PLGA NPs prepared by the double-emulsion/solvent evaporation method, the encapsulation efficiency was increased by two-fold; moreover, the release of gemcitabine was slower, and more potent cytotoxicity was observed against the MCF-7 human breast cancer cells.

3.2. Lipid NPs

Lipid NPs (LNPs) or liposomes can be used to deliver hydrophobic drugs by encapsulating them in the lipid bilayer.⁷⁵ LNPs have become the most clinically advanced nonviral vectors to deliver therapeutic nucleic acids of small interfering RNA (siRNA), messenger RNA (mRNA) or plasmid DNA (pDNA) as more than ten LNP-siRNA/mRNA/pDNA formulations have entered the stage of clinal trials. 76-78 LNP formulations for codelivery of siRNA and mRNA have also been explored; these may enable the simultaneous knockdown of undesirable protein(s) and expression of desirable protein(s).⁷⁹ Moreover, lipid-covered polymeric NPs and pure drug NPs have shown great benefits in drug delivery for their high efficiency and minor side effects. 80,81 Batch methods to produce LNPs involve the stepwise mixing of the lipid-containing organic solution and the nucleic acid-containing aqueous solution to precipitate LNPs, which is generally achieved by extrusion or pipette mixing. The manufacturing challenge for batch methods lies in the poor control of the LNP properties, especially LNP sizes of greater than 100 nm.79 Microfluidic strategies have been applied to reduce the LNP size and size dispersity, and improve the encapsulation efficiency of therapeutic reagents.

The microfluidic synthesis of LNPs, including lipid-coated NPs, can be performed in different types of microfluidic mixers including a SHM, HFF, 3D HFF with microvortices, and T-junction mixers. Producing LNPs using the SHM device has successfully overcome the main hurdle of the batch stepwise mixing of the high-cost tens of milliliters of nucleic acid solution. 44,82 Fig. 5A shows details of a study that developed the SHM method for the synthesis of LNPs which managed to lower the requirement for the volume of input solutions from milliliters to microliters, thus saving expensive siRNA reagents. 44 As little as 10 μL of organic and aqueous solutions were reliably mixed in milliseconds. Compared to the pipette mixing method, which produced LNPs of ~180 nm in diameter, the SHM method decreased the LNP size to below 100 nm. The LNP size was highly reproducible between repeated experiments and was further decreased to ~70 nm at flow rates of 12-60 mL h⁻¹. Moreover, the SHM method enabled improved screening of lipid-like materials for siRNA delivery due to its rapid and small-scale manner. The crucial role of size control of LNPs in siRNA delivery efficiency was shown in another study. 45 Large LNPs of 170 nm in diameter had poor gene silencing in vivo compared to small LNPs of 60 nm in diameter produced by the SHM method. The ability

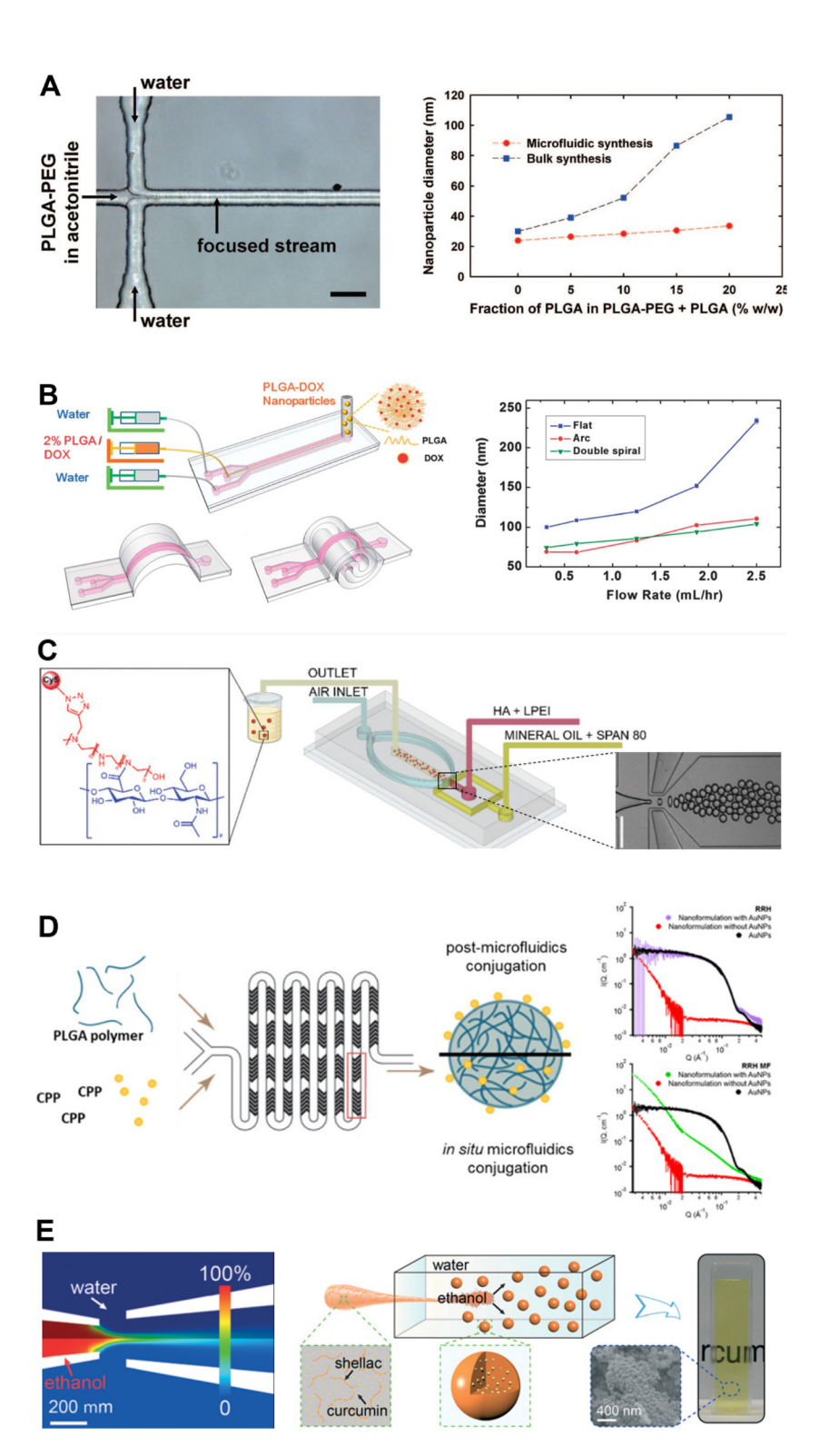


Fig. 4 Microfluidic methods for the synthesis of polymeric NPs. (A) Hydrodynamic flow focusing (HFF). Improved polymeric NP properties by HFF synthesis with a much lower increase in particle size with an increase in PLGA concentration compared to batch NPs (<50% versus >200%), leading to a longer half-life of the encapsulated drug docetaxel. Reprinted with permission from ref. 23. Copyright 2008 American Chemical Society. (B) Spiral HFF. Combination of HFF and 3D curved microchannels achieves good size control of PLGA NPs at ten times higher throughput compared to the flat chip. The half-life is tens of times longer than the free drug curcumin. Reprinted with permission from ref. 70. Copyright 2014 Royal Society of Chemistry. (C) Micro-droplet generator. Highly monodisperse polymeric NPs are formed within the micro-droplets with a very small PDI of 0.015. Reprinted with permission from ref. 72. Copyright 2022 Royal Society of Chemistry. (D) Staggered herringbone micromixer (SHM). PLGA NPs prepared with the SHM show improved in-particle distribution of the encapsulated CPPs. Reprinted with permission from ref. 73. Copyright 2019 Elsevier. (E) Glass capillary. The short mixing time of 9 ms in the glass capillary device enables a high encapsulation efficiency of 98% for curcumin. Reprinted with permission from ref. 58. Copyright 2019 Royal Society of Chemistry.

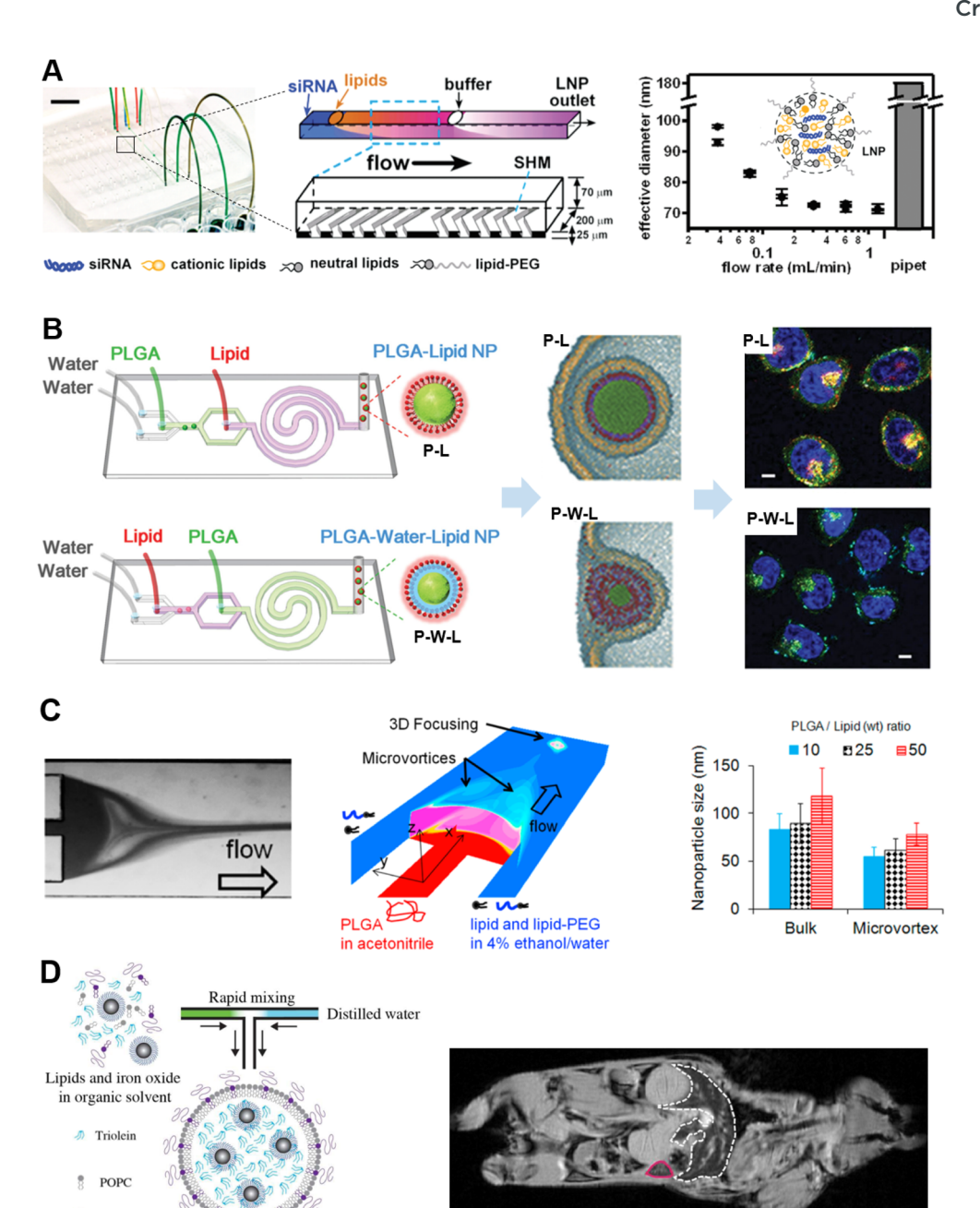


Fig. 5 Microfluidic methods for the synthesis of lipid nanoparticles (LNPs). (A) Staggered herringbone micromixer (SHM). The LNP synthesis by SHM reduces the required volume of input solutions from milliliters to microliters, and decreases the particle size from approximately 180 to 70 nm. Reprinted with permission from ref. 44. Copyright 2012 American Chemical Society. (B) Hydrodynamic flow focusing (HFF). A two-stage HFF device assembles NPs with a lipid shell–polymer core structure, and regulates the cellular take up of NPs by their rigidity, which leads to different dynamics of entry into the cell. Reprinted with permission from ref. 83. Copyright 2014 Wiley. (C) 3D HFF with microvortices. The 3D focusing by microvortices is generated at a Reynolds number of up to 150, achieving reduced particle size and PDI (55–80 nm, 0.1) compared to the batch method (80–120 nm, 0.2). Reprinted with permission from ref. 53. Copyright 2013 American Chemical Society. (D) T-junction mixer. The turbulent T-junction mixer operating at a high Reynolds number of 11 000 scales up LNP production, and the encapsulation of iron oxide NPs into LNPs enhances the image contrast for magnetic resonance imaging (MRI) of the liver (dotted white line) and spleen (pink solid line). Reprinted with permission from ref. 50. Copyright 2017 Royal Society of Chemistry.

of SHM devices to precisely and reproducibly control the LNP size enabled researchers to further study the effect of LNP size on gene silencing by preparing siRNA-loaded LNPs of different sizes ranging from 27 to 117 nm. ²⁴ It was found

PEG-DSPE

that 27 nm LNPs were unstable, and 117 nm LNPs failed to transport through the liver vasculature. The LNPs of 38–78 nm in diameter resulted in the most efficient hepatic gene silencing.

Critical Review Analyst

As shown in Fig. 5B, researchers used a two-stage HFF to assemble NPs with a PLGA core/lipid shell structure.83 The lipid shell could be monolayer (P-L) or bilayer (P-W-L) solely depending on the injection order of PLGA and lipid solutions. The P-L and P-W-L NPs had different rigidity but the same composition, surface chemistry, and size. The cellular take up of NPs was found to be regulated by rigidity. The rigid P-L NP was internalized smoothly, but the less rigid P-W-L NP significantly deformed during internalization, which impeded its entry into the cell. As a result, the HeLa cells took up more "hard" P-L NPs than "soft" P-W-L NPs, as indicated by the higher fluorescence intensities of the cells incubated with the P-L NPs. Fig. 5C shows the production of PLGA-lipid NPs with superior reproducibility and homogeneity using the 3D HFF device with microvortices.⁵³ The device operated at Reynolds numbers of 30-150 yielding a high throughput up to 3 g h⁻¹. The NP size was well controlled in the range of 55-80 nm with a small PDI of ~0.1. In comparison, the batch method produced larger NPs of 80-120 nm in diameter with a PDI of ~0.2. The production of LNPs can be conducted with a turbulent T-junction mixer at a high throughput (Fig. 5D).⁵⁰ Rapid mixing was induced by having the two fluids flow directly toward each other with a perpendicular turbulent output, which required a high Reynolds number of 11 000. Size modulation over the range of 35-150 nm was fulfilled by varying the flow and the core-to-surface lipid ratio. The encapsulation of iron oxide NPs into LNPs provided enhanced image contrast for magnetic resonance imaging (MRI) of the liver and spleen. The turbulent T-junction mixer offers an approach to scale up LNP production; however, it may not be a preferred method for applications such as the high throughput screening of various LNP formulations since it cannot be scaled down to handle small volumes of expensive reagents such as nucleic acids or lipids.

3.3. Inorganic NPs

Inorganic NPs typically possess unique optical properties enabling them to respond to specific external stimuli including light, magnetic field, ultrasound, radiofrequency, and radiation, as well as internal stimuli such as pH, interstitial pressure, and conjugation of biomarkers.84-87 Hence, inorganic NPs have been widely used as therapeutic, diagnostic, or imaging agents. Gold NPs (AuNPs), having a unique surface plasmon resonance (SPR), are one of the most studied types of inorganic NPs. Modulating the optical and photothermal properties of AuNPs has showing promising applications for clinical use such as in tumor imaging,88 tumor ablation,89 and ondemand release of incorporated therapeutics. 90 Iron oxide NPs (IONPs) are another type of inorganic NP that has been extensively investigated because of the uniqueness of the innate magnetic response. IONPs are able to facilitate the combination of imaging with therapy, called theranostics, allowing for more precise drug delivery. 91,92 IONPs can serve as therapeutic agents via magnetic hyperthermia in an alternating magnetic field. The local increase in heat can be used to induce cancer cell death, as well as the triggered release of the

loaded drug. 93,94 Silica (SiO2) NPs (SNPs) are also attractive for drug delivery as not only their size and shape, but also their porosity and the chemical properties of their surfaces can be controlled, which gives them the ability to store and release both hydrophilic and hydrophobic drugs. 95-97 Inorganic NPs are commonly produced by chemical methods (such as chemical reduction) to induce NP precipitation. Batch methods face significant challenges for scaled up production. Batch methods are not able to separate the nanoprecipitation stages of nucleation and growth leading to the problem of high levels of batch-to-batch variation of NP size.

Microfluidic devices such as the micro-droplet generator, glass capillary, and T-junction mixer have been developed for the synthesis or surface modification of inorganic NPs. Fig. 6A shows details of one study using a micro-droplet generator to synthesize silver NPs. 98 The silver salt (silver nitrate) solution was flow focused with another aqueous solution containing the reducing agent tannic acid and the stabilizing agent trisodium citrate forming a series of micro-droplets. The droplet volume could be modulated within 30-80 pL by varying the input flow rates. The experimental results in Fig. 6A illustrate the mixing inside droplets via the observation of the fluorescence of the tracer rhodamine B. A mixing efficiency of 85% was achieved within 40 ms, which was considered fast enough for the precipitation reaction and NP formation. Details of another study utilizing a micro-droplet generator to synthesize silver and gold NPs are shown in Fig. 6B. 99,100 The micro-droplets were generated by a T junction. The droplet contained ionic liquid solutions of the metal salt precursor and the reductant. The gold NPs synthesized by the micro-droplet method were 29% smaller than those from the batch method. More striking differences were observed for silver NPs, which had a well-defined spherical shape in the microfluidic synthesis but appeared as large coral-like assemblies in the batch synthesis.

The study outlined in Fig. 6C used a microfluidic glass capillary device to conduct the surface modification of silicon NPs with a polymer matrix. 101 Both silicon and gold NPs were encapsulated in the polymer matrix by tailoring the NPs' surface properties. The therapeutic compound XMU-MP-1 was also loaded into the porous silicon NPs via nanoprecipitation in the glass capillary. This nanohybrid showed potential as a theranostic reagent for acute liver failure (ALF). The microfluidic synthesized NPs increased the local drug concentration in the lesion area of the liver and enhanced the CT signal to generate a distinguishable area in CT images by the accumulation of NPs in mice with ALF. Fig. 6D shows details of a study to create biomimetic cell membrane-coated NPs via the surface modification of iron oxide NPs (IONPs). 102 Microfluidic mixing between the IONPs and the blood cell membrane-derived vesicles (RBC vesicles) were fulfilled using a variant of a T-junction mixer involving a series of U-shaped turns followed by an electroporation zone. The two reagents were observed to be evenly mixed after the third U turn. This core-shell nano-formulation of RBC-IONPs had magnetic and photothermal properties because of the IONP core, and long blood circulation times

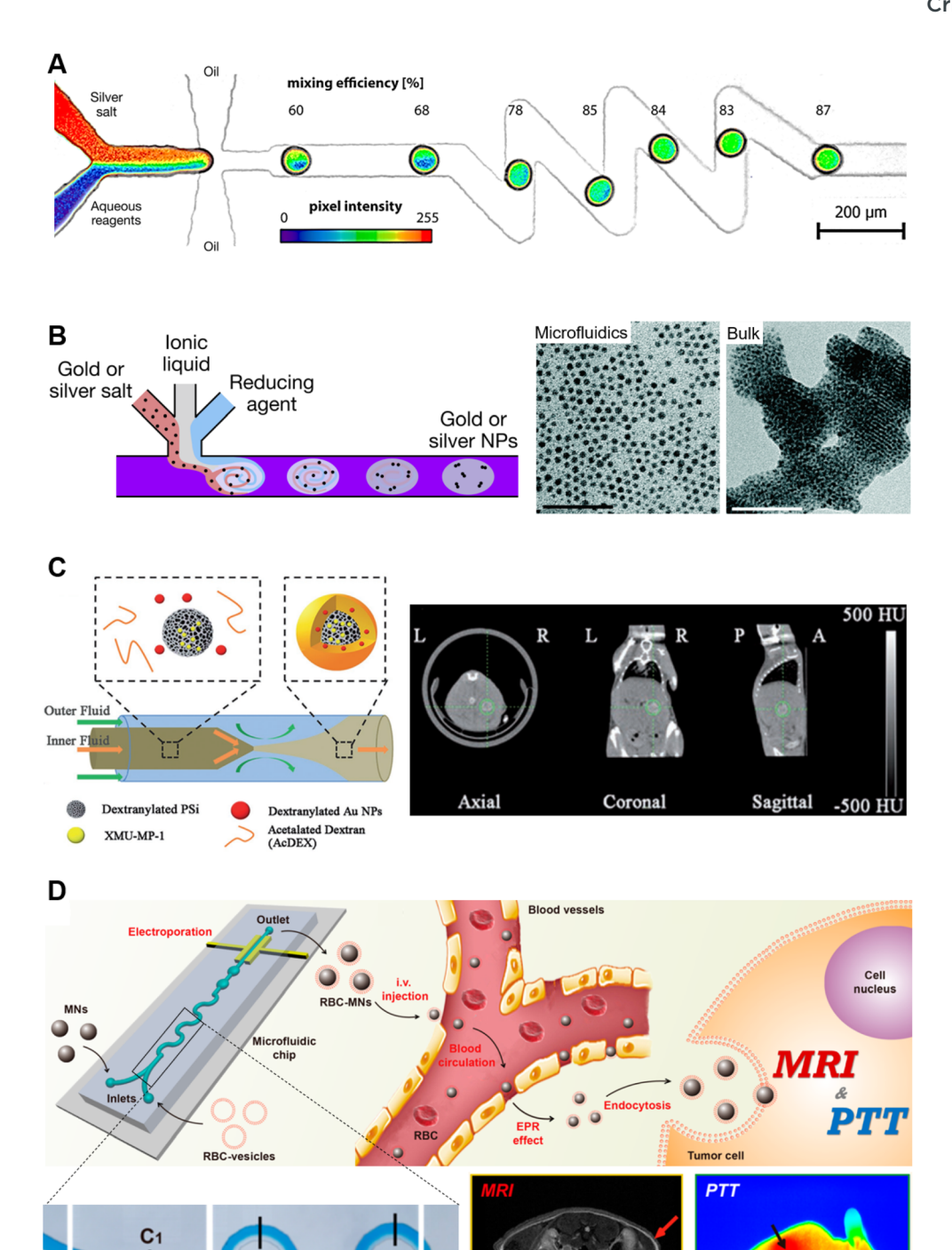


Fig. 6 Microfluidic methods for the synthesis and surface modification of inorganic NPs. (A) Micro-droplet generator (by flow focusing). Efficiency of in-droplet mixing between the silver salt and reducing reagent reaches 85% within 40 ms for a homogeneous precipitation reaction and silver NP formation. Reprinted with permission from ref. 98. Copyright 2019 Springer. (B) Micro-droplet generator (by T junction). Gold NPs are generated in micro-droplets with a well-defined spherical shape and are 29% smaller than those obtained with the batch method. Reprinted with permission from ref. 99 and 100. Copyright 2012 American Chemical Society. Copyright 2021 Elsevier. (C) Glass capillary. Surface modification of silicon NPs with a polymer matrix is conducted in a glass capillary device, and this microfluidically synthesized nanohybrid serves as a theranostic reagent with increased local drug concentration in the lesion area of the liver. Reprinted with permission from ref. 101. Copyright 2017 Wiley. (D) T-junction mixer. The utilization of U-shaped turns after the T-junction enhances the mixing of iron oxide NPs and the surface modification material of blood cell membrane-derived vesicles, and the core-shell nanohybrid exhibits enhanced efficiency for tumor magnetic resonance imaging (MRI) and photothermal therapy (PTT). Reprinted with permission from ref. 102. Copyright 2017 American Chemical Society.

1 mm

owing to the RBC shell. Thus, the RBC-IONPs were used for enhanced tumor magnetic resonance imaging (MRI) and photothermal therapy (PTT) while the microfluidically prepared NPs showed significantly better treatment effects than batch-prepared NPs.

3.4. Drug nanocrystals

Nowadays, a large portion of drugs are designed and generated as poorly water-soluble molecules; this results in the majority of failures in new drug development. 103,104 Specifically, more than 40% of drugs are classified as low solubility drugs by the biopharmaceutical classification system (BCS), 105 and approximately 70-90% of new drugs have the problem of poor aqueous solubility. 106 The incorporation of hydrophobic drugs into NPs enables a faster dissolution rate and higher saturation concentration of the drugs in aqueous solutions. 107,108 Thus, as a drug carrier, NPs improve the solubility and bioavailability of encapsulated drugs. The bioactivity and stability of encapsulated drugs can also be enhanced by protection from the NPs against rapid metabolism and clearance. 109,110 Moreover, the nano-formulation can contribute to lower toxicity and improved therapeutic efficacy of a drug via the spatiotemporal control of drug release. 111-114

Drug nanocrystals, also called pure drug NPs, are a versatile tool for the delivery of hydrophobic drugs as a simple coreshell nanostructure. The drug nanocore is formed first, and then encapsulated by a shell/layer of stabilizer. Polymers and surface-active agents are the most commonly used stabilizers for pharmaceutical nanocrystals. Stabilizers influence not only the stability but also the bioavailability of nanocrystals. For example, Pluronic-grafted chitosan copolymer, as the stabilizer of paclitaxel (PTX) nanocrystals, improved the relative bioavailability of PTX by 12.6-fold compared to TaxolTM. ¹¹⁵ Among the various nano-formulations, the advantages of drug nanocrystals include high drug loading, low preparation cost, and flexible administration routes. 116 Drug nanocrystals are referred to as a nanosuspension when they are suspended in aqueous medium. 104 Apart from conventional clinical or preclinical oral delivery of hydrophobic drugs, drug nanocrystals can be more broadly used via other administration routes, namely, transdermal, pulmonary, ophthalmic, buccal, and intravenous. 117-120

The top-down milling method is not possible or requires a very long process to reduce the size of drug nanocrystals below 100 nm. For example, using the media milling technique, fenofibrate nanocrystals with the stabilizers Soluplus® and HPMC were produced with sizes of 344 nm and 642 nm, respectively. 121 The bottom-up microfluidic nanoprecipitation method can help to reduce the size of drug nanocrystals. Fig. 7A shows a commonly used microfluidic device of a Y-junction mixer to synthesize a hydrocortisone nanosuspension. The ethanolic drug solution was mixed with an aqueous solution containing stabilizers and then introduced into a bulk solution of phosphate buffered saline (PBS) containing stabilizers under continuous sonication. A hydrocortisone nanosuspension with a mean size of 295 ± 32 nm was gener-

ated, which was comparable to the minimum size of hydrocortisone nanocrystals produced by the wet milling method (milling time up to 105 min). The Y-junction mixer was also adopted in other studies to synthesize nanocrystals of different hydrophobic drugs, namely, danazol, 122 cefuroxime axetil, 123 and atorvastatin calcium. 124 These drug nanocrystals produced by Y-junction mixers were generally larger than 300 nm in size. Drug nanocrystals of rubrene smaller than 100 nm were prepared with a HFF device, as shown in Fig. 7B. 125 The ethanolic rubrene solution was focused in the HFF configuration by stabilizer-containing aqueous flows. Efficient diffusion in the region of the focused drug-containing stream was confirmed by confocal fluorescence microscopy in the presence of fluorescein. Rubrene nanocrystals of 50-110 nm in mean diameter were produced by the HFF device by controlling the aqueousto-organic flow ratio. Nanocrystals of paclitaxel (PTX) and sorafenib (SFN) stabilized by the coating polymer hypromellose acetate succinate (HF) were generated with controlled sizes of 60-450 nm and 70-550 nm, respectively, in a study utilizing a glass capillary device for drug nanocrystal synthesis (Fig. 7C). 126 To reduce the nanocrystal size below 100 nm, a high Reynolds number of Re > 500 was required. A dropletbased microfluidic approach was also proposed to synthesize drug nanocrystals of curcumin. 127 As shown in Fig. 7D, the ethanolic curcumin solution was mixed with an aqueous solution containing stabilizers in a T-junction mixer, and then formed hanging droplets from the micro-channel in the openair environment. Simultaneous mixing was activated by inherent chaotic advection within each droplet, which was observed via planar laser-induced fluorescence. As a result, curcumin nanocrystals of 190-450 nm in mean diameter were generated by this droplet-based method depending on the concentration of curcumin.

A surface stabilizer is necessary for drug nanocrystal stabilization; however, grafting ligands to the surface of nanocrystals made of pure drug molecules is technically challenging due to the lack of chemical functional groups. Fig. 7E shows the combination of ionic surfactants and polymeric stabilizers for drug nanocrystal stabilization, which utilize the ionic surfactants for electrostatic repulsion and the polymeric stabilizers for steric hindrance. 104 A recently employed coating material of metal-phenolic networks (MPNs) for drug nanocrystal stabilization is shown in Fig. 7F. 128 MPNs are supramolecular structures formed by the rapid coordination of natural polyphenols (such as tannic acid (TA), gallic acid (GA), and epigallocatechin gallate (EGCG)) with metal ions (such as Fe³⁺, Al³⁺, Sr²⁺, and Cu²⁺). 129,130 MPNs are flexible and compatible with other biomaterials, so they have been developed for the delivery of imaging and therapeutic agents. 129,131-135 MPNs are also non-cytotoxic and degradable making them attractive for the encapsulation of proteinosomes, microbes, and mammalian cells. 136-138 Recently, MPNs were employed as a coating material for drug nanocrystal stabilization. As a thin shell, MPNs can achieve a high drug loading; moreover, MPNs can provide a functionalized surface for the nanocrystal to graft other ligands. 128,139,140 MPN-coated nanocrystals have been

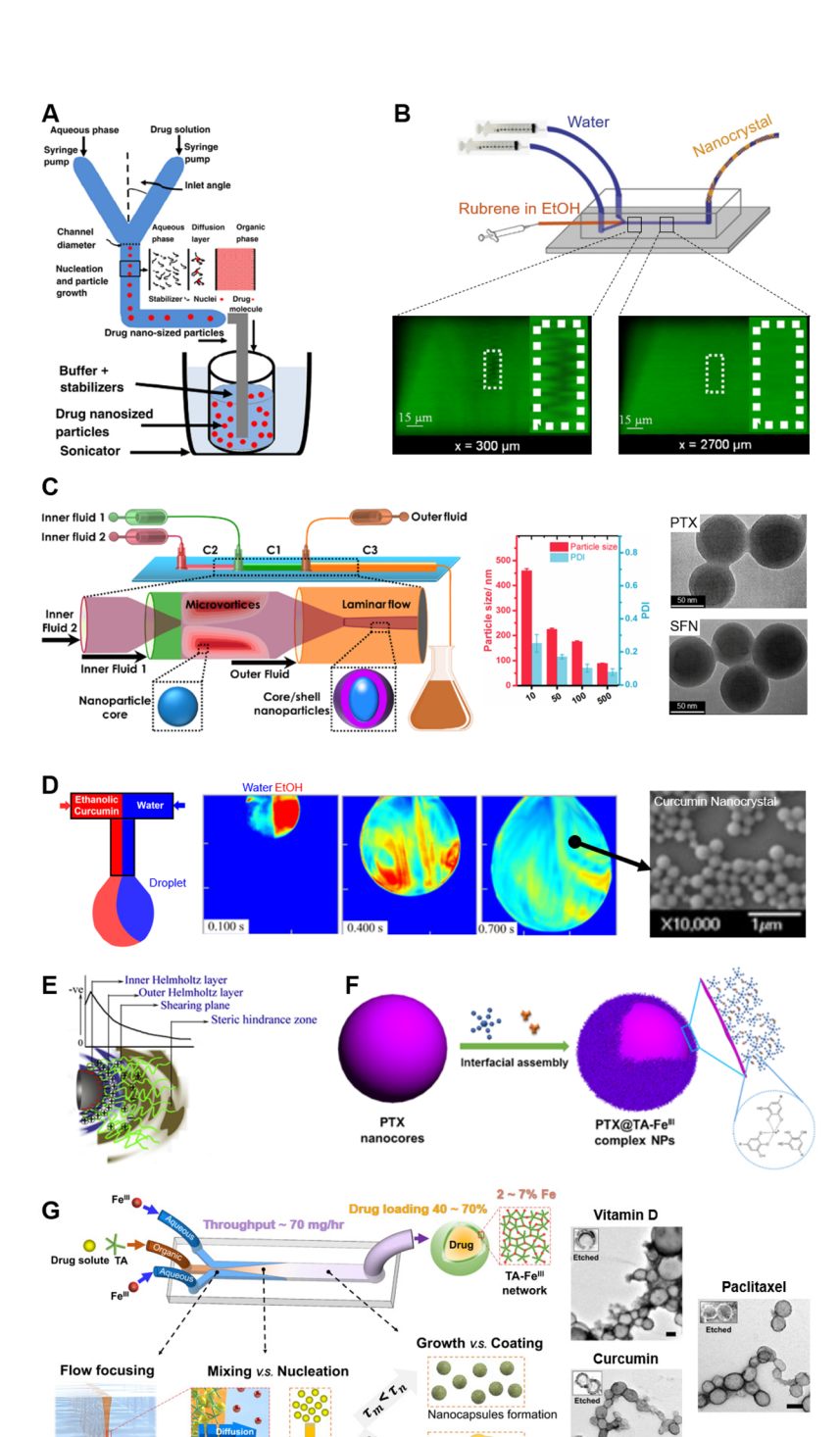


Fig. 7 Microfluidic methods for the synthesis of drug nanocrystals (pure drug NPs). (A) Y-junction mixer. As the simplest bottom-up microfluidic nanoprecipitation method, the Y-junction mixer with the aid of sonication can produce nanocrystals of the hydrophobic drug hydrocortisone with a diameter of ~300 nm. Reprinted with permission from ref. 147. Copyright 2011 Elsevier. (B) Hydrodynamic flow focusing (HFF). The 3D flow focusing device enables fast diffusion of the central stream and thus generates rubrene nanocrystals smaller than 100 nm. Reprinted with permission from ref. 125. Copyright 2010 Elsevier. (C) Glass capillary. Nanocrystals of paclitaxel (PTX) and sorafenib (SFN) smaller than 100 nm are synthesized under conditions of Re > 500. Reprinted with permission from ref. 126. Copyright 2017 American Chemical Society. (D) T-junction mixer followed by inner-droplet mixing. Mixing by inherent chaotic advection within the hanging droplet enables the production of curcumin nanocrystals smaller than 200 nm. Reprinted with permission from ref. 127. Copyright 2010 Springer. (E) Combined with the electrostatic repulsion provided by ionic surfactants, polymer molecules serve as the surface stabilizer for drug nanocrystal stabilization by providing an additional steric hindrance zone. Reprinted with permission from ref. 104. Copyright 2013 Elsevier. (F) Metal-phenolic (Fe³⁺-tannic acid (TA)) network (MPN) as a stabilizer for drug nanocrystals of PTX. Reprinted with permission from ref. 128. Copyright 2016 American Chemical Society. (G) A timescale-guided microfluidic HFF method for the synthesis of MPN-coated nanocrystals of different hydrophobic drugs: PTX, vitamin D, and curcumin. Reprinted with permission from ref. 39. Copyright 2023 Elsevier.

6

Few nanocapsules

thin organic stream

Critical Review Analyst

produced by batch nanoprecipitation methods for the hydrophobic drugs paclitaxel, ¹²⁸ carfilzomib, ¹³⁹ vitamin D, ¹⁴⁰ curcumin, ¹⁴¹ rapamycin, ¹⁴² chlorin e6, ¹⁴³ SN-38, ¹⁴⁴ simvastatin, ¹⁴⁵ andrographolide, 145 and cabazitaxel. 146 Batch methods involve manual pipette mixing and the postprocessing step of sonication; this makes it time-consuming and labor-intensive work for scale up from benchtop production to higher volume batches. Lately, our group developed a microfluidic HFF method for the synthesis of MPN-coated nanocrystals of hydrophobic drugs.³⁹ As shown in Fig. 7G, the mechanism of encapsulating a variety of hydrophobic drugs is established based on the timescales of microfluidic mixing and drug nucleation. Microfluidically synthesized MPN-coated nanocrystals of vitamin D, curcumin, and paclitaxel had well-controlled sizes of 80-200 nm, high drug loadings of 40-70%, and a throughput of up to 70 mg h⁻¹ per channel exhibiting scale-up potential.

3.5. Microfluidic separation and purification of nano-drugs and biologics

In recent decades, microfluidic techniques have advanced to manipulate nanoscale bioparticles, including trapping, 148,149 focusing 150,151 and separation 152 using various forces such as acoustic radiation, ¹⁵³ elastic lift, ¹⁵⁴ dielectrophoresis ^{155–157} as well as inertial and viscous. 158 Fluid properties are relevant to particle separation, namely, viscosity (resistance to flow), density, and fluid velocity. Laminar flow (Re < 2000) not only occurs but also Stokes flow (Re « 1) in the microfluidic channel. Particles in a flow experience shear and normal stresses, generating parallel forces (drag force) and perpendicular forces (wall effect and shear gradient lift forces) to the main flow direction and are aligned in the equilibrium position in

Fig. 8A. 159 Drag forces generally accelerate particles until they reach flow speed equilibrium. 160 In passive separation technologies, particles are controlled by hydrodynamic flow in microfluidics, while active separation technologies involve external forces such as magnetic, acoustic, optical, or electrical effects, often necessitating additional microchannel equipment. 161 In active separation technologies, particle behavior is intricately governed by external forces. For instance, as depicted in Fig. 8B, particle movement is controlled by a magnetic force. 162 When a particle is suspended within a uniform electric field, its movement is significantly influenced by the gradients within a non-uniform electric field, ultimately resulting in a net force (Fig. 8C). 163 Furthermore, surface acoustic waves (SAWs) are generated by a transducer called an interdigital transducer (IDT) and particle movements are affected by SAWs, as shown in Fig. 8D. 164 The separation and purification of nano-drugs and biologics, such as liposomes, viruses, DNA nano-balls, and extracellular vesicles (EVs), are essential prerequisites for their biomedical applications. 165-168 Both passive and active techniques including acoustofluidics, ^{169–171} hydrodynamics, ^{172–174} and dielectrophoresis (DEP)^{175–179} have been employed for the separation and purification of these substances.

Acoustofluidic technologies make use of acoustic waves to precisely control fluids and particles immersed in fluids, which enables contact-free and biocompatible separation of NPs. Particles containing liquid are given motion by the created density, velocity, or pressure field as a result of the acoustic waves propagating in a liquid. The transducer utilized for surface acoustic wave (SAW) generation and reception is called an interdigital transducer (IDT). Fig. 9A shows the design of a stereo acoustic stream (SteAS) for NP separation. 169

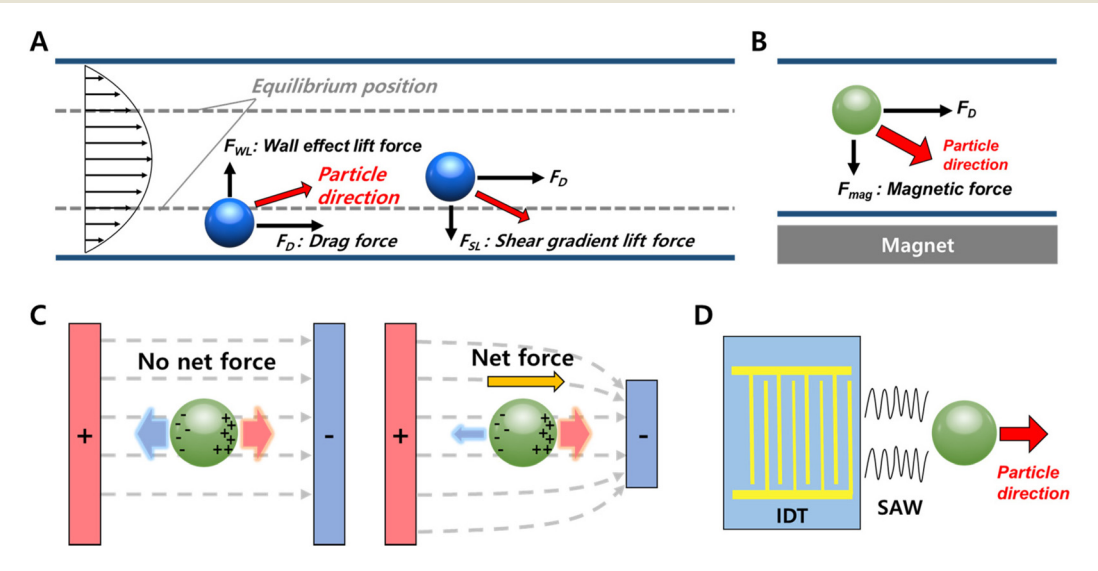


Fig. 8 Particle separation technologies. (A) Hydrodynamic force. Particles move to the equilibrium position and are aligned by parallel forces (drag force) and perpendicular forces (wall effect and shear gradient lift forces). (B) Magnetic force. The direction of particle movement is controlled by a magnetic force, pulling the particles towards the magnet. (C) Electric force. The gradients of a non-uniform electric field lead to a net force and thus control the movement of a suspended particle. (D) Acoustic force. Interdigital transducers (IDTs) generate surface acoustic waves (SAWs) to modulate particle motion.

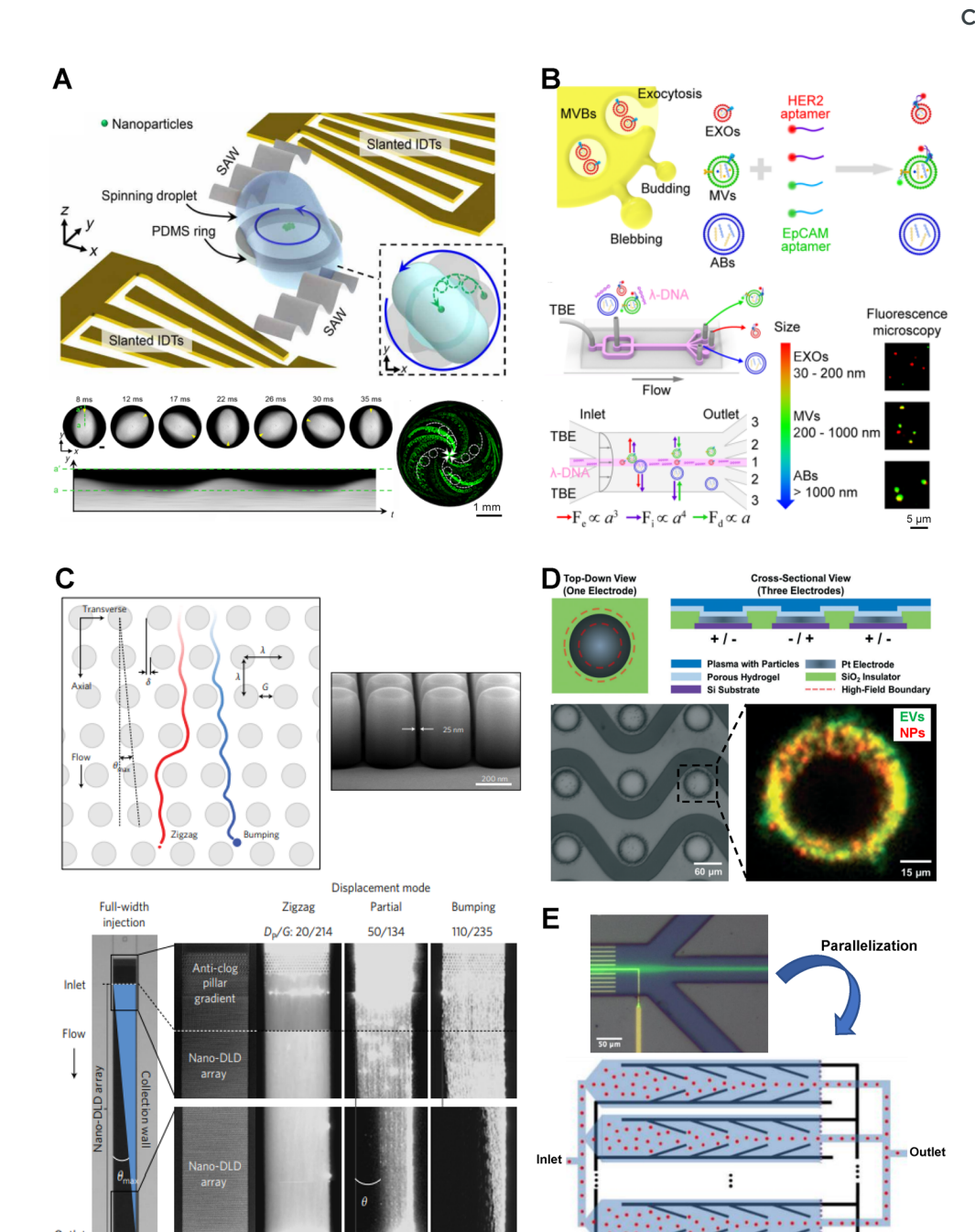


Fig. 9 Microfluidic strategies for separation and purification of nano-sized particles. (A) Acoustofluidics. Operational principles of an acoustofluidic centrifuge platform and dynamics of droplet spinning and particle manipulation within the droplet. Reprinted with permission from ref. 169. (B) Viscoelastic hydrodynamics. Process of size-selective separation of extracellular vesicle (EV) subpopulations through implementation of λ -DNA mediated viscoelastic microfluidics. Reprinted with permission from ref. 173. Copyright 2019 American Chemical Society. (C) Nanoscale deterministic lateral displacement (nano-DLD) arrays for NP separation. Reprinted with permission from ref. 152. Copyright 2016 Springer. (D) Dielectrophoresis (DEP) for stagnant fluids. An example shows the collection of polystyrene NPs (red) and EVs (green) by DEP arrays. Reprinted with permission from ref. 177. Copyright 2021 American Chemical Society. (E) DEP for continuous flows. Sub-100 nm polymer particles (green) focused in the center of channel, as well as the parallelization design. Reprinted with permission from ref. 176.

A droplet is placed on a PDMS ring located between two IDTs. The SteAS makes the droplet start to spin as the surface acoustic waves (SAWs) propagate into the droplet. Then the particles within the spinning droplet migrate toward its center, following a dual-axis rotational trajectory. The SteAS was able to

capture 30 nm polystyrene NPs and continuously focus 150 nm polystyrene NPs. This acoustofluidic technology enables the enrichment and continuous size-based separation of NPs, and thus holds potential for applications in analytical chemistry and nano-drugs.

Critical Review Analyst

The hydrodynamics method for NP separation can utilize viscoelastic microfluidics to manipulate NPs in a more precise manner than inertial microfluidics. 172,173 Viscoelasticityinduced microfluidic devices have been utilized to focus and separate particles. Fig. 9B shows the design of viscoelastic microfluidics mediated by λ -DNA and aptamers, by which EV subpopulations are size-selectively separated. 173 The cellderived EVs include exosomes (EXOs), microvesicles (MVs), and apoptotic bodies (ABs), which can utilize aptamers specific to HER2 and EpCAM. EXOs with sizes below 200 nm were submerged in the viscoelastic sample fluid, experiencing the centerline-directed elastic lift force. Conversely, MVs and ABs with sizes equal to or exceeding 200 nm were repelled by the force exerted by the flow, leading them to migrate towards the Newtonian sheath stream devoid of elasticity. Thus, these three EV subpopulations were separated for surface protein analysis of individual EVs. The panel of aptamers for the multiple detection of EV markers can be expanded, and the diagnostic value of EV subpopulations for different types of cancer can be further studied using this viscoelastic microfluidics.

The hydrodynamics method of deterministic lateral displacement (DLD) employs pillar arrays to continuously separate particles based on their size. The pillar arrays induce fluid bifurcation and result in a distinctive number of streamlines within the gaps. Particles that are smaller than the critical diameter follow the streamlines in zigzag mode (migration angle $\theta = \theta_{\text{max}}$), otherwise the particles behave differently in bumping mode ($\theta = 0$), or the mode of partial displacement (0 $<\theta<\theta_{\rm max}$). Fig. 9C shows the design of nanoscale deterministic lateral displacement (nano-DLD) arrays with consistent gap sizes ranging from 25 to 235 nm. 152 These nano-DLD arrays effectively separated particles within the size range of 20 to 110 nm with sharp resolution. This hydrodynamics method of nano-DLD enables continuous and rapid NP sorting with single-particle resolution without the need for particle labelling. On-chip sorting and the quantification of biocolloids, such as EVs, can also be fulfilled using the DLD technique.

Dielectrophoresis (DEP) refers to the movement of an object by DEP forces; specifically, when an object is suspended in a fluid and exposed to a non-uniform electric field, the contrasting dielectric properties between the object and its surrounding medium result in the generation of DEP forces acting on the object. 175,181,182 Fig. 9D shows the measurement of fluorescence intensity of EVs from blood plasma (green) and polystyrene NPs (blue) captured on the surface of DEP regions within a microfluidic device. 177 This optical DEP technique can be adapted to other lab-on-a-chip platforms that feature the analysis of cancer-related biomarkers. Fig. 9E shows another example of DEP microfluidics achieving the increased concentration and sorting of NPs in a continuous flow. The sub-100 nm particles (green fluorescence) were focused towards the center of the channel and directed towards the center outlet by the DEP force from a DC field. For the parallelization of channels utilizing the DEP force from an AC field, the inclined microsized electrodes in a zigzag threetooth pattern were found to generate the largest DEP force to

focus the NPs with diameters of 84 or 47 nm. The massive parallelization of this DEP microfluidics can increase throughput by a factor of 1250, which shows the potential for applications in clinical diagnosis and nano-drug purification.

4. Summary

The success of microfluidic techniques in dealing with the batch-to-batch variations of batch synthesis methods for nanoformulations relies on the small scale of microfluidic mixing, which makes the precises control of rapid diffusive mass transfer possible. The micrometer scale of microfluidics enables a short mixing time, as well as uniform mixing flow patterns, yielding the small size and narrow size distribution of the microfluidically synthesized NPs. However, scaling up the microfluidic throughput to the industrial level is challenging. It is notable that the microfluidic flow capacity, Q, dramatically decreases with a decrease in the channel size, h, due to the increase of the hydraulic resistance, RH, which can be expressed as $Q \propto R^{-1}_{H} \propto h^{4}$. For example, the flow capacity may be 80 times higher with a 3 times longer microfluidic channel (e.g. 300 µm versus 100 µm). Thus, although the continuous-flow manner makes microfluidic techniques promising for large-scale production, it would still be meaningful to estimate the maximum microfluidic channel size for the synthesis of nano-formulations, guided by the timescale-based mechanism of mixing time versus precipitation time during the nanoprecipitation process.

Microfluidic channels can be prepared from a variety of materials such as polymers, glass, and silicon. Polymers are currently the most promising materials for microfluidic devices due to the advantages of flexibility, versatility, and biocompatibility, among which polydimethylsiloxane (PDMS) is undoubtedly the most widely used material. 183-185 Efforts are also made in the development of alternative materials beyond PDMS, such as non-binding polymers or plastics, due to PDMS's non-specific adsorption of proteins and other small molecule drugs. $^{186-189}$ The microchannel geometry can be prepared by soft lithography and other lithography techniques such as reactive-ion etching, electron-beam lithography, and direct laser writing. 190-193 The preparation of microfluidic devices can also be conducted by 3D printing or laser cutting as potential approaches for commercialization. 194,195 However, the high entry level due to the required knowledge of fluid dynamics, and the preparation of complex configurations of microfluidics, still hinder the utilization of microfluidics by broader research and industrial communities.

Despite the challenges discussed above, the development of microfluidics is rapidly evolving to solve current problems and expand to future directions. For example, one of the main issues of channel clogging is being addressed by 3D HFF and glass capillary techniques, and the scaling up of throughput to the industrial level by the parallelization of microfluidic devices is promising. ^{196,197} For future directions, the development of integrated microfluidic synthesis and separation

devices with in-line characterization and control set-ups 198 is highly desirable, as these would enable real-time monitoring and in-process adjustment to optimize the production quality of nano-formulations. Microfluidics is also a modular manufacturing technology for the future decentralized approach to nanomedicine manufacturing, which may facilitate the design and production of nanomedicines to meet local or individual needs; for example, the development of microfluidics may deal with strained mRNA-LNP production, which has caused shortages of vaccines. 199 For now, the microfluidic technique is more developed for NP synthesis, while drug delivery evaluation of the synthesized nano-formulation requires the development of new platforms or techniques for nanomedicine. Many nano-formulations showed satisfactory delivery in vitro, but failed when it came to in vivo environments.200-202 One main challenge in drug delivery evolution is a modular platform that maintains necessary physicochemical properties which the conventional 2D monolayer cell culture system cannot provide. 203-205 The combination of microfluidic techniques for the NP synthesis platform, as well as a NP delivery evaluation platform, such as the tumor-on-a-chip models of pancreatic cancer and breast cancer developed in our lab,206-209 can play an important role in pre-clinical phase trials for nanoparticle-based drug formulation development.

Conflicts of interest

There are no conflicts to declare.

Acknowledgements

This study was partially supported by grants from NIH (R01 CA254110 and U01 CA274304), NSF (MCB-2134603), the Purdue University Institute for Cancer Research (P30 CA023168), and a Program Grant from the Purdue Institute for Drug Discovery.

References

- 1 M. Germain, F. Caputo, S. Metcalfe, G. Tosi, K. Spring, A. K. O. Åslund, A. Pottier, R. Schiffelers, A. Ceccaldi and R. Schmid, Delivering the power of nanomedicine to patients today, J. Controlled Release, 2020, 326, 164-171.
- 2 R. van der Meel, E. Sulheim, Y. Shi, F. Kiessling, W. J. M. Mulder and T. Lammers, Smart cancer nanomedicine, Nat. Nanotechnol., 2019, 14, 1007-1017.
- 3 I. de Lázaro and D. J. Mooney, Obstacles and opportunities in a forward vision for cancer nanomedicine, Nat. Mater., 2021, 20, 1469-1479.
- 4 S. J. Shepherd, D. Issadore and M. J. Mitchell, Microfluidic formulation of nanoparticles for biomedical applications, Biomaterials, 2021, 274, 120826.

- 5 S. Bisso and J.-C. Leroux, Nanopharmaceuticals: A focus on their clinical translatability, Int. J. Pharm., 2020, 578,
- 6 L. A. Jackson, E. J. Anderson, N. G. Rouphael, Roberts, M. Makhene, R. N. Coler, M. P. McCullough, J. D. Chappell, M. R. Denison and L. J. Stevens, An mRNA vaccine against SARS-CoV-2-preliminary report, N. Engl. J. Med., 2020, 383, 1920-1931.
- 7 L. Milane and M. Amiji, Clinical approval of nanotechnology-based SARS-CoV-2 mRNA vaccines: impact on translational nanomedicine, Drug Delivery Transl. Res., 2021, 11, 1309-1315.
- 8 J. S. Thomas, D. Habib, D. L. Hanna, I. Kang, S. Iqbal, J. J. Nieva, D. Tsao-Wei, F. Acosta, M. Hsieh and Y. Zhang, in A phase 1 trial of FID-007, a novel nanoparticle paclitaxel formulation, in patients with solid tumors, Wolters Kluwer Health, 2021.
- 9 Z. A. Wainberg, H. S. Hochster, E. J. Kim, B. George, Kaylan, E. G. Chiorean, D. M. Waterhouse, M. Guiterrez, A. Parikh and R. Jain, Open-label, phase I study of nivolumab combined with nab-paclitaxel plus gemcitabine in advanced pancreatic cancer, Clin. Cancer Res., 2020, 26, 4814-4822.
- 10 S. M. Stavis, J. A. Fagan, M. Stopa and J. A. Liddle, Nanoparticle manufacturing-heterogeneity through processes to products, ACS Appl. Nano Mater., 2018, 1, 4358-
- 11 S. Mülhopt, S. Diabaté, M. Dilger, C. Adelhelm, C. Anderlohr, T. Bergfeldt, J. Gómez de la Torre, Y. Jiang, E. Valsami-Jones and D. Langevin, Characterization of nanoparticle batch-to-batch variability, Nanomaterials, 2018, 8, 311.
- 12 A. Zielińska, F. Carreiró, A. M. Oliveira, A. Neves, B. Pires, D. N. Venkatesh, A. Durazzo, M. Lucarini, P. Eder and A. M. Silva, Polymeric nanoparticles: production, characterization, toxicology and ecotoxicology, Molecules, 2020, **25**, 3731.
- 13 S. Bohrey, V. Chourasiya and A. Pandey, Polymeric nanoparticles containing diazepam: preparation, optimization, characterization, in vitro drug release and release kinetic study, Nano Convergence, 2016, 3, 1-7.
- 14 Y. Yang, Y. Ding, B. Fan, Y. Wang, Z. Mao, W. Wang and J. Wu, Inflammation-targeting polymeric nanoparticles deliver sparfloxacin and tacrolimus for combating acute lung sepsis, J. Controlled Release, 2020, 321, 463-474.
- 15 S. C. Semple, A. Akinc, J. Chen, A. P. Sandhu, B. L. Mui, C. K. Cho, D. W. Y. Sah, D. Stebbing, E. J. Crosley and E. Yaworski, Rational design of cationic lipids for siRNA delivery, Nat. Biotechnol., 2010, 28, 172-176.
- 16 A. Bagde, K. Patel, S. Kutlehria, N. Chowdhury and M. Singh, Formulation of topical ibuprofen solid lipid nanoparticle (SLN) gel using hot melt extrusion technique (HME) and determining its anti-inflammatory strength, Drug Delivery Transl. Res., 2019, 9, 816-827.
- 17 J. Hu, W. K. Ng, Y. Dong, S. Shen and R. B. H. Tan, Continuous and scalable process for water-redispersible

nanoformulation of poorly aqueous soluble APIs by antisolvent precipitation and spray-drying, *Int. J. Pharm.*, 2011, **404**, 198–204.

- 18 Y. Lu, Y. Li and W. Wu, Injected nanocrystals for targeted drug delivery, *Acta Pharm. Sin. B*, 2016, **6**, 106–113.
- 19 K. M. R. Srivalli and B. Mishra, Drug nanocrystals: A way toward scale-up, *Saudi Pharm. J.*, 2016, **24**, 386–404.
- 20 F. Alexis, E. Pridgen, L. K. Molnar and O. C. Farokhzad, Factors affecting the clearance and biodistribution of polymeric nanoparticles, *Mol. Pharm.*, 2008, 5, 505–515.
- 21 M. A. Dobrovolskaia, P. Aggarwal, J. B. Hall and S. E. McNeil, Preclinical studies to understand nanoparticle interaction with the immune system and its potential effects on nanoparticle biodistribution, *Mol. Pharm.*, 2008, 5, 487–495.
- 22 X. Huang, L. Li, T. Liu, N. Hao, H. Liu, D. Chen and F. Tang, The shape effect of mesoporous silica nanoparticles on biodistribution, clearance, and biocompatibility in vivo, *ACS Nano*, 2011, 5, 5390–5399.
- 23 R. Karnik, F. Gu, P. Basto, C. Cannizzaro, L. Dean, W. Kyei-Manu, R. Langer and O. C. Farokhzad, Microfluidic platform for controlled synthesis of polymeric nanoparticles, *Nano Lett.*, 2008, 8, 2906–2912.
- 24 S. Chen, Y. Y. C. Tam, P. J. C. Lin, M. M. H. Sung, Y. K. Tam and P. R. Cullis, Influence of particle size on the in vivo potency of lipid nanoparticle formulations of siRNA, *J. Controlled Release*, 2016, 235, 236–244.
- 25 S. G. M. Ong, M. Chitneni, K. S. Lee, L. C. Ming and K. H. Yuen, Evaluation of extrusion technique for nanosizing liposomes, *Pharmaceutics*, 2016, **8**, 36.
- 26 D. B. Shelar, S. K. Pawar and P. R. Vavia, Fabrication of isradipine nanosuspension by anti-solvent microprecipitation-high-pressure homogenization method for enhancing dissolution rate and oral bioavailability, *Drug Delivery Transl. Res.*, 2013, 3, 384–391.
- 27 Y. Le, H. Ji, J.-F. Chen, Z. Shen, J. Yun and M. Pu, Nanosized bicalutamide and its molecular structure in solvents, *Int. J. Pharm.*, 2009, 370, 175–180.
- 28 X. Zhang, Q. Xia and N. Gu, Preparation of all-trans retinoic acid nanosuspensions using a modified precipitation method, *Drug Dev. Ind. Pharm.*, 2006, 32, 857–863.
- 29 P. M. Valencia, O. C. Farokhzad, R. Karnik and R. Langer, Microfluidic technologies for accelerating the clinical translation of nanoparticles, *Nano-Enabled Med. Appl.*, 2020, 93–112.
- 30 K. Zhai, X. Pei, C. Wang, Y. Deng, Y. Tan, Y. Bai, B. Zhang, K. Xu and P. Wang, Water-in-oil Pickering emulsion polymerization of N-isopropyl acrylamide using starch-based nanoparticles as emulsifier, *Int. J. Biol. Macromol.*, 2019, **131**, 1032–1037.
- 31 A. Fabozzi, F. Della Sala, M. di Gennaro, M. Barretta, G. Longobardo, N. Solimando, M. Pagliuca and A. Borzacchiello, Design of functional nanoparticles by microfluidic platforms as advanced drug delivery systems for cancer therapy, *Lab Chip*, 2023, 23, 1389–1409.

- 32 R. J. Davey, S. L. M. Schroeder and J. H. Ter Horst, Nucleation of organic crystals—a molecular perspective, *Angew. Chem., Int. Ed.*, 2013, 52, 2166–2179.
- 33 J. Polte, R. Erler, A. F. Thunemann, S. Sokolov, T. T. Ahner, K. Rademann, F. Emmerling and R. Kraehnert, Nucleation and growth of gold nanoparticles studied via in situ small angle X-ray scattering at millisecond time resolution, ACS Nano, 2010, 4, 1076– 1082.
- 34 S. Teychené and B. Biscans, Nucleation kinetics of polymorphs: induction period and interfacial energy measurements, *Cryst. Growth Des.*, 2008, **8**, 1133–1139.
- 35 N. T. K. Thanh, N. Maclean and S. Mahiddine, Mechanisms of nucleation and growth of nanoparticles in solution, *Chem. Rev.*, 2014, **114**, 7610–7630.
- 36 H. Yang, M. Svard, J. Zeglinski and Å.C Rasmuson, Influence of solvent and solid-state structure on nucleation of parabens, *Cryst. Growth Des.*, 2014, 14, 3890–3902.
- 37 D. J. Jin, H. S. Uhm and G. Cho, Influence of the gas-flow Reynolds number on a plasma column in a glass tube, *Phys. Plasmas*, 2013, 20, 083513.
- 38 D. Holzinger and A. Ehresmann, Diffusion enhancement in a laminar flow liquid by near-surface transport of superparamagnetic bead rows, *Microfluid. Nanofluid.*, 2015, 19, 395–402.
- 39 Y. Shen, S. A. Yuk, S. Kwon, H. Tamam, Y. Yeo and B. Han, A timescale-guided microfluidic synthesis of tannic acid-FeIII network nanocapsules of hydrophobic drugs, *J. Controlled Release*, 2023, 357, 484–497.
- 40 K. K. F. Glass, E. K. Longmire and A. Hubel, Optimization of a microfluidic device for diffusion-based extraction of DMSO from a cell suspension, *Int. J. Heat Mass Transfer*, 2008, **51**, 5749–5757.
- 41 M. Lu, A. Ozcelik, C. L. Grigsby, Y. Zhao, F. Guo, K. W. Leong and T. J. Huang, Microfluidic hydrodynamic focusing for synthesis of nanomaterials, *Nano Today*, 2016, **11**, 778–792.
- 42 D. Holcman and Z. Schuss, Time scale of diffusion in molecular and cellular biology, *J. Phys. A: Math. Theor.*, 2014, 47, 173001.
- 43 G.-B. Lee, C.-C. Chang, S.-B. Huang and R.-J. Yang, The hydrodynamic focusing effect inside rectangular microchannels, *J. Micromech. Microeng.*, 2006, 16, 1024.
- 44 D. Chen, K. T. Love, Y. Chen, A. A. Eltoukhy, C. Kastrup, G. Sahay, A. Jeon, Y. Dong, K. A. Whitehead and D. G. Anderson, Rapid discovery of potent siRNA-containing lipid nanoparticles enabled by controlled microfluidic formulation, *J. Am. Chem. Soc.*, 2012, 134, 6948–6951.
- 45 N. M. Belliveau, J. Huft, P. J. C. Lin, S. Chen, A. K. K. Leung, T. J. Leaver, A. W. Wild, J. B. Lee, R. J. Taylor and Y. K. Tam, Microfluidic synthesis of highly potent limit-size lipid nanoparticles for in vivo delivery of siRNA, Mol. Ther.-Nucleic Acids, 2012, 1, e37.
- 46 A. D. Stroock, S. K. W. Dertinger, A. Ajdari, I. Mezic, H. A. Stone and G. M. Whitesides, Chaotic mixer for microchannels, *Science*, 2002, 295, 647–651.

- 47 M. Maeki, T. Saito, Y. Sato, T. Yasui, N. Kaji, A. Ishida, H. Tani, Y. Baba, H. Harashima and M. Tokeshi, A strategy for synthesis of lipid nanoparticles using microfluidic devices with a mixer structure, RSC Adv., 2015, 5, 46181– 46185.
- 48 A. Abou-Hassan, O. Sandre and V. Cabuil, Microfluidics in inorganic chemistry, *Angew. Chem., Int. Ed.*, 2010, 49, 6268–6286.
- 49 S. Thomas, T. Ameel and J. Guilkey, Mixing kinematics of moderate Reynolds number flows in a T-channel, *Phys. Fluids*, 2010, **22**, 013601.
- 50 J. A. Kulkarni, Y. Y. C. Tam, S. Chen, Y. K. Tam, J. Zaifman, P. R. Cullis and S. Biswas, Rapid synthesis of lipid nanoparticles containing hydrophobic inorganic nanoparticles, *Nanoscale*, 2017, 9, 13600–13609.
- 51 M. A. Ansari, K.-Y. Kim, K. Anwar and S. M. Kim, Vortex micro T-mixer with non-aligned inputs, *Chem. Eng. J.*, 2012, **181**, 846–850.
- 52 M. A. Ansari, K.-Y. Kim and S. M. Kim, Numerical and experimental study on mixing performances of simple and vortex micro T-mixers, *Micromachines*, 2018, **9**, 204.
- 53 Y. Kim, B. Lee Chung, M. Ma, W. J. M. Mulder, Z. A. Fayad, O. C. Farokhzad and R. Langer, Mass production and size control of lipid-polymer hybrid nanoparticles through controlled microvortices, *Nano Lett.*, 2012, 12, 3587–3591.
- 54 Y. Kim, F. Fay, D. P. Cormode, B. L. Sanchez-Gaytan, J. Tang, E. J. Hennessy, M. Ma, K. Moore, O. C. Farokhzad and E. A. Fisher, Single step reconstitution of multifunctional high-density lipoprotein-derived nanomaterials using microfluidics, *ACS Nano*, 2013, 7, 9975–9983.
- 55 M. Rhee, P. M. Valencia, M. I. Rodriguez, R. Langer, O. C. Farokhzad and R. Karnik, Synthesis of size-tunable polymeric nanoparticles enabled by 3D hydrodynamic flow focusing in single-layer microchannels, *Adv. Mater.*, 2011, 23, H79-H83.
- 56 X. Luo, P. Su, W. Zhang and C. L. Raston, Microfluidic devices in fabricating nano or micromaterials for biomedical applications, *Adv. Mater. Technol.*, 2019, 4, 1900488.
- 57 G. Gkogkos, M. O. Besenhard, L. Storozhuk, N. T. K. Thanh and A. Gavriilidis, Fouling-proof triple stream 3D flow focusing based reactor: Design and demonstration for iron oxide nanoparticle co-precipitation synthesis, *Chem. Eng. Sci.*, 2022, 251, 117481.
- 58 L. Kong, R. Chen, X. Wang, C.-X. Zhao, Q. Chen, M. Hai, D. Chen, Z. Yang and D. A. Weitz, Controlled co-precipitation of biocompatible colorant-loaded nanoparticles by microfluidics for natural color drinks, *Lab Chip*, 2019, 19, 2089–2095.
- 59 R. Othman, G. T. Vladisavljević, H. C. H. Bandulasena and Z. K. Nagy, Production of polymeric nanoparticles by micromixing in a co-flow microfluidic glass capillary device, *Chem. Eng. J.*, 2015, 280, 316–329.
- 60 J. Wang, W. Chen, J. Sun, C. Liu, Q. Yin, L. Zhang, Y. Xianyu, X. Shi, G. Hu and X. Jiang, A microfluidic

- tubing method and its application for controlled synthesis of polymeric nanoparticles, *Lab Chip*, 2014, **14**, 1673–1677.
- 61 K.-I. Min, H.-J. Lee and D.-P. Kim, Three-dimensional flash flow microreactor for scale-up production of monodisperse PEG-PLGA nanoparticles, *Lab Chip*, 2014, 14, 3987–3992.
- 62 D. Desai, Y. A. Guerrero, V. Balachandran, A. Morton, L. Lyon, B. Larkin and D. E. Solomon, Towards a microfluidics platform for the continuous manufacture of organic and inorganic nanoparticles, *Nanomedicine*, 2021, 35, 102402.
- 63 D. Prochowicz, A. Kornowicz and J. Lewiński, Interactions of native cyclodextrins with metal ions and inorganic nanoparticles: fertile landscape for chemistry and materials science, *Chem. Rev.*, 2017, 117, 13461– 13501.
- 64 X. Li and X. Jiang, Microfluidics for producing poly (lactic-co-glycolic acid)-based pharmaceutical nanoparticles, Adv. Drug Delivery Rev., 2018, 128, 101–114.
- 65 H. K. Makadia and S. J. Siegel, Poly lactic-co-glycolic acid (PLGA) as biodegradable controlled drug delivery carrier, *Polymers*, 2011, 3, 1377–1397.
- 66 E. Sah and H. Sah, Recent trends in preparation of poly (lactide-co-glycolide) nanoparticles by mixing polymeric organic solution with antisolvent, *J. Nanomater.*, 2015, 16, 61–61.
- 67 S. Zalba, T. L. M. Ten Hagen, C. Burgui and M. J. Garrido, Stealth nanoparticles in oncology: Facing the PEG dilemma, J. Controlled Release, 2022, 351, 22–36.
- 68 H. H. Gustafson, D. Holt-Casper, D. W. Grainger and H. Ghandehari, Nanoparticle uptake: the phagocyte problem, *Nano Today*, 2015, 10, 487–510.
- 69 N. Kamaly, B. Yameen, J. Wu and O. C. Farokhzad, Degradable controlled-release polymers and polymeric nanoparticles: mechanisms of controlling drug release, *Chem. Rev.*, 2016, 116, 2602–2663.
- 70 J. Sun, Y. Xianyu, M. Li, W. Liu, L. Zhang, D. Liu, C. Liu, G. Hu and X. Jiang, A microfluidic origami chip for synthesis of functionalized polymeric nanoparticles, *Nanoscale*, 2013, 5, 5262–5265.
- 71 M. H. M. Leung and A. Q. Shen, Microfluidic assisted nanoprecipitation of PLGA nanoparticles for curcumin delivery to leukemia jurkat cells, *Langmuir*, 2018, 34, 3961–3970.
- 72 S. M. Giannitelli, E. Limiti, P. Mozetic, F. Pinelli, X. Han, F. Abbruzzese, F. Basoli, D. Del Rio, S. Scialla and F. Rossi, Droplet-based microfluidic synthesis of nanogels for controlled drug delivery: tailoring nanomaterial properties via pneumatically actuated flow-focusing junction, *Nanoscale*, 2022, 14, 11415–11428.
- 73 S. Streck, A. J. Clulow, H. M. Nielsen, T. Rades, B. J. Boyd and A. McDowell, The distribution of cell-penetrating peptides on polymeric nanoparticles prepared using microfluidics and elucidated with small angle X-ray scattering, J. Colloid Interface Sci., 2019, 555, 438–448.

74 L. Martín-Banderas, E. Sáez-Fernández, M.Á Holgado, M. M. Durán-Lobato, J. C. Prados, C. Melguizo and J. L. Arias, Biocompatible gemcitabine-based nanomedicine engineered by Flow Focusing® for efficient anti-

- tumor activity, *Int. J. Pharm.*, 2013, **443**, 103–109.

 75 L. Sercombe, T. Veerati, F. Moheimani, S. Y. Wu, A. K. Sood and S. Hua, Advances and challenges of liposome assisted drug delivery, *Front. Pharmacol.*, 2015, **6**, 286.
- 76 M. J. W. Evers, J. A. Kulkarni, R. van der Meel, P. R. Cullis, P. Vader and R. M. Schiffelers, State-of-the-art design and rapid-mixing production techniques of lipid nanoparticles for nucleic acid delivery, *Small Methods*, 2018, 2, 1700375.
- 77 Y. Sato, Y. Note, M. Maeki, N. Kaji, Y. Baba, M. Tokeshi and H. Harashima, Elucidation of the physicochemical properties and potency of siRNA-loaded small-sized lipid nanoparticles for siRNA delivery, *J. Controlled Release*, 2016, 229, 48–57.
- 78 Y. Zhu, R. Shen, I. Vuong, R. A. Reynolds, M. J. Shears, Z.-C. Yao, Y. Hu, W. J. Cho, J. Kong and S. K. Reddy, Multi-step screening of DNA/lipid nanoparticles and codelivery with siRNA to enhance and prolong gene expression, *Nat. Commun.*, 2022, 13, 4282.
- 79 R. L. Ball, K. A. Hajj, J. Vizelman, P. Bajaj and K. A. Whitehead, Lipid Nanoparticle Formulations for Enhanced Co-delivery of siRNA and mRNA, *Nano Lett.*, 2018, 18, 3814–3822.
- 80 P. M. Valencia, P. A. Basto, L. Zhang, M. Rhee, R. Langer, O. C. Farokhzad and R. Karnik, Single-step assembly of homogenous lipid—polymeric and lipid—quantum dot nanoparticles enabled by microfluidic rapid mixing, ACS Nano, 2010, 4, 1671–1679.
- 81 D. Xia, Y. He, Q. Li, C. Hu, W. Huang, Y. Zhang, F. Wan, C. Wang and Y. Gan, Transport mechanism of lipid covered saquinavir pure drug nanoparticles in intestinal epithelium, *J. Controlled Release*, 2018, 269, 159–170.
- 82 Y. Wu, B. Yu, A. Jackson, W. Zha, L. J. Lee and B. E. Wyslouzil, Coaxial electrohydrodynamic spraying: a novel one-step technique to prepare oligodeoxynucleotide encapsulated lipoplex nanoparticles, *Mol. Pharm.*, 2009, 6, 1371–1379.
- 83 J. Sun, L. Zhang, J. Wang, Q. Feng, D. Liu, Q. Yin, D. Xu, Y. Wei, B. Ding and X. Shi, Tunable rigidity of (polymeric core)-(lipid shell) nanoparticles for regulated cellular uptake, *Adv. Mater.*, 2014, 27, 1402–1407.
- 84 S. Veeranarayanan and T. Maekawa, External stimulus responsive inorganic nanomaterials for cancer theranostics, *Adv. Drug Delivery Rev.*, 2019, **138**, 18–40.
- 85 A. C. Anselmo and S. Mitragotri, A review of clinical translation of inorganic nanoparticles, *AAPS J*, 2015, **17**, 1041–1054.
- 86 N. Hao, Y. Nie and J. X. J. Zhang, Microfluidic synthesis of functional inorganic micro-/nanoparticles and applications in biomedical engineering, *Int. Mater. Rev.*, 2018, 63, 461–487.

- 87 J. Shen, M. Shafiq, M. Ma and H. Chen, Synthesis and surface engineering of inorganic nanomaterials based on microfluidic technology, *Nanomaterials*, 2020, **10**, 1177.
- 88 A. Meola, J. Rao, N. Chaudhary, M. Sharma and S. D. Chang, Gold nanoparticles for brain tumor imaging: A systematic review, *Front. Neurol.*, 2018, **9**, 328.
- 89 H. B. Ruttala, T. Ramasamy, B. K. Poudel, R. R. T. Ruttala, S. G. Jin, H.-G. Choi, S.-K. Ku, C. S. Yong and J. O. Kim, Multi-responsive albumin-lonidamine conjugated hybridized gold nanoparticle as a combined photothermal-chemotherapy for synergistic tumor ablation, *Acta Biomater.*, 2020, **101**, 531–543.
- 90 M. Malki, A. Shapira and T. Dvir, Chondroitin sulfate-AuNRs electroactive scaffolds for on-demand release of biofactors, J. Nanobiotechnol., 2022, 20, 1–9.
- 91 I. Ternad, S. Penninckx, V. Lecomte, T. Vangijzegem, L. Conrard, S. Lucas, A.-C. Heuskin, C. Michiels, R. N. Muller and D. Stanicki, Advances in the Mechanistic Understanding of Iron Oxide Nanoparticles' Radiosensitizing Properties, *Nanomaterials*, 2023, 13, 201.
- 92 A. Setia, A. K. Mehata, A. K. Malik, M. K. Viswanadh and M. S. Muthu, Theranostic magnetic nanoparticles: Synthesis, properties, toxicity, and emerging trends for biomedical applications, *J. Drug Delivery Sci. Technol.*, 2023, 104295.
- 93 A. Włodarczyk, S. Gorgoń, A. Radoń and K. Bajdak-Rusinek, Magnetite Nanoparticles in Magnetic Hyperthermia and Cancer Therapies: Challenges and Perspectives, *Nanomaterials*, 2022, **12**, 1807.
- 94 A. A. Demessie, Y. Park, P. Singh, A. S. Moses, T. Korzun, F. Y. Sabei, H. A. Albarqi, L. Campos, C. R. Wyatt and K. Farsad, An Advanced Thermal Decomposition Method to Produce Magnetic Nanoparticles with Ultrahigh Heating Efficiency for Systemic Magnetic Hyperthermia, *Small Methods*, 2022, 6, 2200916.
- 95 Y. Chen, H. Chen, M. Ma, F. Chen, L. Guo, L. Zhang and J. Shi, Double mesoporous silica shelled spherical/ellipsoidal nanostructures: synthesis and hydrophilic/hydrophobic anticancer drug delivery, *J. Mater. Chem.*, 2011, 21, 5290–5298.
- 96 A. A. Alhowyan, M. A. Kalam, M. Iqbal, M. Raish, A. M. El-Toni, M. Alkholief, A. A. Almomen and A. Alshamsan, Mesoporous silica nanoparticles coated with carboxymethyl chitosan for 5-fluorouracil ocular delivery: characterization, in vitro and in vivo studies, *Molecules*, 2023, 28, 1260.
- 97 J. Yan, X. Xu, J. Zhou, C. Liu, L. Zhang, D. Wang, F. Yang and H. Zhang, Fabrication of a pH/redox-triggered mesoporous silica-based nanoparticle with microfluidics for anticancer drugs doxorubicin and paclitaxel codelivery, ACS Appl. Bio Mater., 2020, 3, 1216–1225.
- 98 O. Kašpar, A. H. Koyuncu, A. Pittermannová, P. Ulbrich and V. Tokárová, Governing factors for preparation of silver nanoparticles using droplet-based microfluidic device, *Biomed. Microdevices*, 2019, **21**, 1–14.

3077-3083.

99 L. L. Lazarus, C. T. Riche, B. C. Marin, M. Gupta, N. Malmstadt and R. L. Brutchey, Two-phase microfluidic droplet flows of ionic liquids for the synthesis of gold and silver nanoparticles, ACS Appl. Mater. Interfaces, 2012, 4,

- 100 S. J. Shepherd, D. Issadore and M. J. Mitchell, Microfluidic formulation of nanoparticles for biomedical applications, *Biomaterials*, 2021, 120826.
- 101 Z. Liu, Y. Li, W. Li, C. Xiao, D. Liu, C. Dong, M. Zhang, E. Mäkilä, M. Kemell and J. Salonen, Multifunctional nanohybrid based on porous silicon nanoparticles, gold nanoparticles, and acetalated dextran for liver regeneration and acute liver failure theranostics, *Adv. Mater.*, 2018, 30, 1703393.
- 102 L. Rao, B. Cai, L.-L. Bu, Q.-Q. Liao, S.-S. Guo, X.-Z. Zhao, W.-F. Dong and W. Liu, Microfluidic electroporation-facilitated synthesis of erythrocyte membrane-coated magnetic nanoparticles for enhanced imaging-guided cancer therapy, ACS Nano, 2017, 11, 3496–3505.
- 103 S. Kalepu and V. Nekkanti, Insoluble drug delivery strategies: review of recent advances and business prospects, *Acta Pharm. Sin. B*, 2015, 5, 442–453.
- 104 B. Sinha, R. H. Müller and J. P. Möschwitzer, Bottom-up approaches for preparing drug nanocrystals: formulations and factors affecting particle size, *Int. J. Pharm.*, 2013, 453, 126–141.
- 105 J. Tao, S. F. Chow and Y. Zheng, Application of flash nanoprecipitation to fabricate poorly water-soluble drug nanoparticles, *Acta Pharm. Sin. B*, 2019, **9**, 4–18.
- 106 A. Tuomela, J. Hirvonen and L. Peltonen, Stabilizing agents for drug nanocrystals: effect on bioavailability, *Pharmaceutics*, 2016, 8, 16.
- 107 J. Xie, Y. Luo, Y. Liu, Y. Ma, P. Yue and M. Yang, Novel redispersible nanosuspensions stabilized by co-processed nanocrystalline cellulose–sodium carboxymethyl starch for enhancing dissolution and oral bioavailability of baicalin, *Int. J. Nanomed.*, 2019, 14, 353.
- 108 Y. Aidana, Y. Wang, J. Li, S. Chang, K. Wang and D.-G. Yu, Fast dissolution electrospun medicated nanofibers for effective delivery of poorly water-soluble drug, *Curr. Drug Delivery*, 2022, **19**, 422–435.
- 109 C. P. Feliciano, K. Tsuboi, K. Suzuki, H. Kimura and Y. Nagasaki, Long-term bioavailability of redox nanoparticles effectively reduces organ dysfunctions and death in whole-body irradiated mice, *Biomaterials*, 2017, **129**, 68–82.
- 110 B.-Q. Chen, Y. Zhao, Y. Zhang, Y.-J. Pan, H.-Y. Xia, R. K. Kankala, S.-B. Wang, G. Liu and A.-Z. Chen, Immune-regulating camouflaged nanoplatforms: A promising strategy to improve cancer nano-immunotherapy, *Bioact. Mater.*, 2023, **21**, 1–19.
- 111 J. H. Lee and Y. Yeo, Controlled drug release from pharmaceutical nanocarriers, *Chem. Eng. Sci.*, 2015, 125, 75–84.
- 112 W. Zuo, D. Chen, Z. Fan, L. Chen, Z. Zhu, Q. Zhu and X. Zhu, Design of light/ROS cascade-responsive tumor-

- recognizing nanotheranostics for spatiotemporally controlled drug release in locoregional photo-chemotherapy, *Acta Biomater.*, 2020, **111**, 327–340.
- 113 H. Guo, J. Huang, Y. Tan, W. Wu, T. Huang, N. Zhang, S. Chen, C. Zhang, X. Xie and X. Shuai, Nanodrug shows spatiotemporally controlled release of anti-PD-L1 antibody and STING agonist to effectively inhibit tumor progression after radiofrequency ablation, *Nano Today*, 2022, 43, 101425.
- 114 C. J. Gil, L. Li, B. Hwang, M. Cadena, A. S. Theus, T. A. Finamore, H. Bauser-Heaton, M. Mahmoudi, R. K. Roeder and V. Serpooshan, Tissue engineered drug delivery vehicles: Methods to monitor and regulate the release behavior, J. Controlled Release, 2022, 349, 143–155.
- 115 S. Sharma, A. Verma, G. Pandey, N. Mittapelly and P. R. Mishra, Investigating the role of Pluronic-g-Cationic polyelectrolyte as functional stabilizer for nanocrystals: Impact on Paclitaxel oral bioavailability and tumor growth, *Acta Biomater.*, 2015, 26, 169–183.
- 116 L. Gao, G. Liu, J. Ma, X. Wang, L. Zhou and X. Li, Drug nanocrystals: in vivo performances, *J. Controlled Release*, 2012, **160**, 418–430.
- 117 M. L. Branham, T. Moyo and T. Govender, Preparation and solid-state characterization of ball milled saquinavir mesylate for solubility enhancement, *Eur. J. Pharm. Biopharm.*, 2012, **80**, 194–202.
- 118 S. Sultana, S. Talegaonkar, R. Ali, G. Mittal, F. J. Ahmad and A. Bhatnagar, Inhalation of alendronate nanoparticles as dry powder inhaler for the treatment of osteoporosis, *J. Microencapsulation*, 2012, **29**, 445–454.
- 119 Y. Lv, W. Wu, C. D. Corpstein, T. Li and Y. Lu, Biological and intracellular fates of drug nanocrystals through different delivery routes: Recent development enabled by bioimaging and PK modeling, *Adv. Drug Delivery Rev.*, 2022, 114466.
- 120 X. Miao, W. Yang, T. Feng, J. Lin and P. Huang, Drug nanocrystals for cancer therapy, *Wiley Interdiscip. Rev.: Nanomed. Nanobiotechnol.*, 2018, **10**, e1499.
- 121 H. Yang, F. Teng, P. Wang, B. Tian, X. Lin, X. Hu, L. Zhang, K. Zhang, Y. Zhang and X. Tang, Investigation of a nanosuspension stabilized by Soluplus® to improve bioavailability, *Int. J. Pharm.*, 2014, 477, 88–95.
- 122 H. Zhao, J.-X. Wang, Q.-A. Wang, J.-F. Chen and J. Yun, Controlled liquid antisolvent precipitation of hydrophobic pharmaceutical nanoparticles in a microchannel reactor, *Ind. Eng. Chem. Res.*, 2007, 46, 8229–8235.
- 123 J.-X. Wang, Q.-X. Zhang, Y. Zhou, L. Shao and J.-F. Chen, Microfluidic synthesis of amorphous cefuroxime axetil nanoparticles with size-dependent and enhanced dissolution rate, *Chem. Eng. J.*, 2010, 162, 844–851.
- 124 H.-X. Zhang, J.-X. Wang, L. Shao and J.-F. Chen, Microfluidic fabrication of monodispersed pharmaceutical colloidal spheres of atorvastatin calcium with tunable sizes, *Ind. Eng. Chem. Res.*, 2010, 49, 4156–4161.
- 125 V. Génot, S. Desportes, C. Croushore, J.-P. Lefèvre, R. B. Pansu, J. A. Delaire and P. R. von Rohr, Synthesis of

organic nanoparticles in a 3D flow focusing microreactor, Chem. Eng. J., 2010, 161, 234-239.

- 126 D. Liu, H. Zhang, S. Cito, J. Fan, E. Mäkilä, J. Salonen, J. Hirvonen, T. M. Sikanen, D. A. Weitz and H. l. A. Santos, Core/shell nanocomposites produced by superfast sequential microfluidic nanoprecipitation, Nano Lett., 2017, 17, 606-614.
- 127 Z. Liu, Y. Huang, Y. Jin and Y. Cheng, Mixing intensification by chaotic advection inside droplets for controlled nanoparticle preparation, Microfluid. Nanofluid., 2010, 9, 773-786.
- 128 G. Shen, R. Xing, N. Zhang, C. Chen, G. Ma and X. Yan, Interfacial cohesion and assembly of bioadhesive molecules for design of long-term stable hydrophobic nanodrugs toward effective anticancer therapy, ACS Nano, 2016, 10, 5720-5729.
- 129 J. Li, Y. Zhou, J. Liu, X. Yang, K. Zhang, L. Lei, H. Hu, H. Zhang, L. Ouyang and H. Gao, Metal-phenolic networks with ferroptosis to deliver NIR-responsive CO for synergistic therapy, J. Controlled Release, 2022, 352, 313-327.
- 130 Y. Chen, W. Xu, M. Shafiq, D. Song, T. Wang, Z. Yuan, X. Xie, X. Yu, Y. Shen and B. Sun, Injectable nanofiber microspheres modified with metal phenolic networks for effective osteoarthritis treatment, Acta Biomater., 2023, **157**, 593-608.
- 131 H. Ejima, J. J. Richardson, K. Liang, J. P. Best, M. P. van Koeverden, G. K. Such, J. Cui and F. Caruso, One-step assembly of coordination complexes for versatile film and particle engineering, Science, 2013, 341, 154-157.
- 132 C. Gao, Y. Wang, Z. Ye, Z. Lin, X. Ma and Q. He, Biomedical Micro-/Nanomotors: From Overcoming Biological Barriers to In Vivo Imaging, Adv. Mater., 2021, 33, 2000512.
- 133 Y. Ping, J. Guo, H. Ejima, X. Chen, J. J. Richardson, H. Sun and F. Caruso, pH-responsive capsules engineered from metal-phenolic networks for anticancer drug delivery, Small, 2015, 11, 2032-2036.
- 134 S. A. Abouelmagd, N. H. Abd Ellah, O. Amen, A. Abdelmoez and N. G. Mohamed, Self-assembled tannic acid complexes for pH-responsive delivery of antibiotics: role of drug-carrier interactions, Int. J. Pharm., 2019, 562, 76-85.
- 135 Z. He, Y. Hu, Z. Gui, Y. Zhou, T. Nie, J. Zhu, Z. Liu, K. Chen, L. Liu and K. W. Leong, Sustained release of exendin-4 from tannic acid/Fe(III) nanoparticles prolongs blood glycemic control in a mouse model of type II diabetes, J. Controlled Release, 2019, 301, 119-128.
- 136 W. Li, W. Bing, S. Huang, J. Ren and X. Qu, Mussel Byssus-Like Reversible Metal-Chelated Supramolecular Complex Used for Dynamic Cellular Surface Engineering and Imaging, Adv. Funct. Mater., 2015, 25, 3775-3784.
- 137 D. Su, X. Liu, L. Wang, C. Ma, H. Xie, H. Zhang, X. Meng, Y. Huang and X. Huang, Bio-inspired engineering proteinosomes with a cell-wall-like protective shell by self-

- assembly of a metal-chelated complex, Chem. Commun., 2016, 52, 13803-13806.
- 138 J. Lee, H. Cho, J. Choi, D. Kim, D. Hong, J. H. Park, S. H. Yang and I. S. Choi, Chemical sporulation and germination: cytoprotective nanocoating of individual mammalian cells with a degradable tannic acid-Fe III complex, Nanoscale, 2015, 7, 18918-18922.
- 139 M. S. Taha, G. M. Cresswell, J. Park, W. Lee, T. L. Ratliff and Y. Yeo, Sustained delivery of carfilzomib by tannic acid-based nanocapsules helps develop antitumor immunity, Nano Lett., 2019, 19, 8333-8341.
- 140 S. A. Yuk, H. Kim, N. S. Abutaleb, A. M. Dieterly, M. S. Taha, M. D. Tsifansky, L. T. Lyle, M. N. Seleem and Y. Yeo, Nanocapsules modify membrane interaction of polymyxin B to enable safe systemic therapy of Gramnegative sepsis, Sci. Adv., 2021, 7, eabj1577.
- 141 Y. Chen, D. Jia, Q. Wang, Y. Sun, Z. Rao, X. Lei, J. Zhao, K. Zeng, Z. Xu and J. Ming, Promotion of the anticancer activity of curcumin based on a metal-polyphenol networks delivery system, Int. J. Pharm., 2021, 602, 120650.
- 142 P. Liu, X. Liu, Y. Cheng, S. Zhong, X. Shi, S. Wang, M. Liu, J. Ding and W. Zhou, Core-Shell Nanosystems for Self-Activated Drug-Gene Combinations against Triple-Negative Breast Cancer, ACS Appl. Mater. Interfaces, 2020, 12, 53654-53664.
- 143 Y. Liu, K. Ma, T. Jiao, R. Xing, G. Shen and X. Yan, Waterinsoluble photosensitizer nanocolloids stabilized by supramolecular interfacial assembly towards photodynamic therapy, Sci. Rep., 2017, 7, 1-8.
- 144 F. Taemaitree, Y. Koseki, N. Saito, R. Suzuki, A. T. N. Dao and H. Kasai, Self-assemble tannic acid and iron complexes on pure nanodrugs surface prevents aggregation and enhances anticancer drug delivery efficiency, Mol. Cryst. Liq. Cryst., 2020, 706, 116-121.
- 145 F. Huang, X. Jiang, M. A. Sallam, X. Zhang and W. He, A Nanocrystal Platform Based on Metal-Phenolic Network Wrapping for Drug Solubilization, AAPS PharmSciTech, 2022, 23, 1-11.
- 146 M. Mu, X. Liang, D. Chuan, S. Zhao, W. Yu, R. Fan, A. Tong, N. Zhao, B. Han and G. Guo, Chitosan coated pH-responsive metal-polyphenol delivery platform for melanoma chemotherapy, Carbohydr. Polym., 2021, 264, 118000.
- 147 H. S. M. Ali, P. York, A. M. A. Ali and N. Blagden, Hydrocortisone nanosuspensions for ophthalmic delivery: a comparative study between microfluidic nanoprecipitation and wet milling, J. Controlled Release, 2011, 149, 175-
- 148 S. D. Ibsen, J. Wright, J. M. Lewis, S. Kim, S. Y. Ko, J. Ong, S. Manouchehri, A. Vyas, J. Akers, C. C. Chen, B. S. Carter, S. C. Esener and M. J. Heller, Rapid Isolation and Detection of Exosomes and Associated Biomarkers from Plasma, ACS Nano, 2017, 11, 6641-6651.
- 149 V. Chaurey, A. Rohani, Y. H. Su, K. T. Liao, C. F. Chou and N. S. Swami, Scaling down constriction-based (electrodeless) dielectrophoresis devices for trapping nanoscale bio-

- particles in physiological media of high-conductivity, *Electrophoresis*, 2013, **34**, 1097–1104.
- 150 M. Dimaki, M. H. Olsen, N. Rozlosnik and W. E. Svendsen, Sub-100 nm Nanoparticle Upconcentration in Flow by Dielectrophoretic Forces, *Micromachines*, 2022, 13, 866.
- 151 C. Liu, J. Y. Guo, F. Tian, N. Yang, F. S. Yan, Y. P. Ding, J. Y. Wei, G. Q. Hu, G. J. Nie and J. S. Sun, Field-Free Isolation of Exosomes from Extracellular Vesicles by Microfluidic Viscoelastic Flows, ACS Nano, 2017, 11, 6968– 6976.
- 152 B. H. Wunsch, J. T. Smith, S. M. Gifford, C. Wang, M. Brink, R. L. Bruce, R. H. Austin, G. Stolovitzky and Y. Astier, Nanoscale lateral displacement arrays for the separation of exosomes and colloids down to 20 nm, *Nat. Nanotechnol.*, 2016, 11, 936–940.
- 153 H. Bruus, Acoustofluidics 7: The acoustic radiation force on small particles, *Lab Chip*, 2012, **12**, 1014–1021.
- 154 A. N. Morozov and W. van Saarloos, An introductory essay on subcritical instabilities and the transition to turbulence in visco-elastic parallel shear flows, *Phys. Rep.*, 2007, 447, 112–143.
- 155 D. Y. Li, W. C. Yu, T. Zhou, M. Q. Li, Y. X. Song and D. Q. Li, Conductivity-difference-enhanced DC dielectrophoretic particle separation in a microfluidic chip, *Analyst*, 2022, 147, 1106–1116.
- 156 W. J. Zhao, L. Q. Zhang, Y. F. Ye, Y. A. Li, X. F. Luan, J. L. Liu, J. Cheng, Y. Zhao, M. X. Li and C. J. Huang, Microsphere mediated exosome isolation and ultra-sensitive detection on a dielectrophoresis integrated microfluidic device, *Analyst*, 2021, 146, 5962–5972.
- 157 S. Ayala-Mar, V. H. Perez-Gonzalez, M. A. Mata-Gomez, R. C. Gallo-Villanueva and J. Gonzalez-Valdez, Electrokinetically Driven Exosome Separation and Concentration Using Dielectrophoretic-Enhanced PDMS-Based Microfluidics, *Anal. Chem.*, 2019, **91**, 14975– 14982.
- 158 T. M. Squires and S. R. Quake, Microfluidics: Fluid physics at the nanoliter scale, *Rev. Mod. Phys.*, 2005, 77, 977–1026.
- 159 D. Di Carlo, Inertial microfluidics, *Lab Chip*, 2009, 9, 3038–3046.
- 160 H. Amini, W. Lee and D. Di Carlo, Inertial microfluidic physics, *Lab Chip*, 2014, 14, 2739–2761.
- 161 S. W. Choe, B. Kim and M. Kim, Progress of Microfluidic Continuous Separation Techniques for Micro-/Nanoscale Bioparticles, *Biosensors*, 2021, **11**, 464.
- 162 P. Su, C. H. Ren, Y. S. Fu, J. H. Guo, J. C. Guo and Q. Yuan, Magnetophoresis in microfluidic lab: Recent advance, *Sens. Actuators*, *A*, 2021, 332, 113180.
- 163 C. Zhang, K. Khoshmanesh, A. Mitchell and K. Kalantarzadeh, Dielectrophoresis for manipulation of micro/nano particles in microfluidic systems, *Anal. Bioanal. Chem.*, 2010, **396**, 401–420.
- 164 Y. Gao, M. R. Wu, Y. Lin and J. Xu, Acoustic Microfluidic Separation Techniques and Bioapplications: A Review, *Micromachines*, 2020, **11**, 921.

- 165 Y. Yang, L. Zhang, K. Jin, M. He, W. Wei, X. Chen, Q. Yang, Y. Wang, W. Pang and X. Ren, Selfadaptive virtual microchannel for continuous enrichment and separation of nanoparticles, *Sci. Adv.*, 2022, 8, eabn8440.
- 166 S. Hettiarachchi, H. Cha, L. Ouyang, A. Mudugamuwa, H. An, G. Kijanka, N. Kashaninejad, N.-T. Nguyen and J. Zhang, Recent microfluidic advances in submicron to nanoparticle manipulation and separation, *Lab Chip*, 2023, 23, 982–1010.
- 167 H. Hu, G. Cai, Z. Gao, C. Liang, F. Yang, X. Dou, C. Jia, J. Zhao, S. Feng and B. Li, A microfluidic immunosensor for automatic detection of carcinoembryonic antigen based on immunomagnetic separation and droplet arrays, *Analyst*, 2023, 148, 1939–1947.
- 168 C. A. Hermann, M. Mayer, C. Griesche, F. Beck and A. J. Baeumner, Microfluidic-enabled magnetic labelling of nanovesicles for bioanalytical applications, *Analyst*, 2021, 146, 997–1003.
- 169 Y. Gu, C. Chen, Z. Mao, H. Bachman, R. Becker, J. Rufo, Z. Wang, P. Zhang, J. Mai and S. Yang, Acoustofluidic centrifuge for nanoparticle enrichment and separation, *Sci.* Adv., 2021, 7, eabc0467.
- 170 J. Rufo, F. Cai, J. Friend, M. Wiklund and T. J. Huang, Acoustofluidics for biomedical applications, *Nat. Rev. Methods Primers*, 2022, 2, 30.
- 171 S. Zhao, M. Wu, S. Yang, Y. Wu, Y. Gu, C. Chen, J. Ye, Z. Xie, Z. Tian and H. Bachman, A disposable acoustofluidic chip for nano/microparticle separation using unidirectional acoustic transducers, *Lab Chip*, 2020, 20, 1298–1308.
- 172 C. Liu, J. Guo, F. Tian, N. Yang, F. Yan, Y. Ding, J. Wei, G. Hu, G. Nie and J. Sun, Field-free isolation of exosomes from extracellular vesicles by microfluidic viscoelastic flows, *ACS Nano*, 2017, **11**, 6968–6976.
- 173 C. Liu, J. Zhao, F. Tian, J. Chang, W. Zhang and J. Sun, λ-DNA-and aptamer-mediated sorting and analysis of extracellular vesicles, *J. Am. Chem. Soc.*, 2019, **141**, 3817–3821.
- 174 M. Asghari, X. Cao, B. Mateescu, D. Van Leeuwen, M. K. Aslan, S. Stavrakis and A. J. deMello, Oscillatory viscoelastic microfluidics for efficient focusing and separation of nanoscale species, ACS Nano, 2019, 14, 422– 433.
- 175 S. Ayala-Mar, V. H. Perez-Gonzalez, M. A. Mata-Gómez, R. C. Gallo-Villanueva and J. González-Valdez, Electrokinetically driven exosome separation and concentration using dielectrophoretic-enhanced PDMS-based microfluidics, *Anal. Chem.*, 2019, **91**, 14975–14982.
- 176 M. Dimaki, M. H. Olsen, N. Rozlosnik and W. E. Svendsen, Sub–100 nm Nanoparticle Upconcentration in Flow by Dielectrophoretic Forces, *Micromachines*, 2022, **13**, 866.
- 177 K. T. Gustafson, K. T. Huynh, D. Heineck, J. Bueno,A. Modestino, S. Kim, A. Gower, R. Armstrong,C. E. Schutt and S. D. Ibsen, Automated fluorescence

quantification of extracellular vesicles collected from blood plasma using dielectrophoresis, *Lab Chip*, 2021, **21**, 1318–1332.

- 178 J. H. Moore, W. B. Varhue, Y.-H. Su, S. S. Linton, V. Farmehini, T. E. Fox, G. L. Matters, M. Kester and N. S. Swami, Conductance-based biophysical distinction and microfluidic enrichment of nanovesicles derived from pancreatic tumor cells of varying invasiveness, *Anal. Chem.*, 2019, **91**, 10424–10431.
- 179 R. Salemmilani, M. Moskovits and C. D. Meinhart, Microfluidic analysis of fentanyl-laced heroin samples by surface-enhanced Raman spectroscopy in a hydrophobic medium, *Analyst*, 2019, **144**, 3080–3087.
- 180 T. Salafi, Y. Zhang and Y. Zhang, A review on deterministic lateral displacement for particle separation and detection, *Nano-Micro Lett.*, 2019, **11**, 1–33.
- 181 D. Li, W. Yu, T. Zhou, M. Li, Y. Song and D. Li, Conductivity-difference-enhanced DC dielectrophoretic particle separation in a microfluidic chip, *Analyst*, 2022, 147, 1106–1116.
- 182 W. Zhao, L. Zhang, Y. Ye, Y. Li, X. Luan, J. Liu, J. Cheng, Y. Zhao, M. Li and C. Huang, Microsphere mediated exosome isolation and ultra-sensitive detection on a dielectrophoresis integrated microfluidic device, *Analyst*, 2021, **146**, 5962–5972.
- 183 A. Shakeri, S. Khan and T. F. Didar, Conventional and emerging strategies for the fabrication and functionalization of PDMS-based microfluidic devices, *Lab Chip*, 2021, 21, 3053–3075.
- 184 J. Zhou, A. V. Ellis and N. H. Voelcker, Recent developments in PDMS surface modification for microfluidic devices, *Electrophoresis*, 2010, 31, 2–16.
- 185 K. J. Regehr, M. Domenech, J. T. Koepsel, K. C. Carver, S. J. Ellison-Zelski, W. L. Murphy, L. A. Schuler, E. T. Alarid and D. J. Beebe, Biological implications of polydimethylsiloxane-based microfluidic cell culture, *Lab Chip*, 2009, 9, 2132–2139.
- 186 M. Radisic and P. Loskill, in *Beyond PDMS and membranes:* new materials for organ-on-a-chip devices, ACS Publications, 2021, pp. 2861–2863.
- 187 S. B. Campbell, Q. Wu, J. Yazbeck, C. Liu, S. Okhovatian and M. Radisic, Beyond polydimethylsiloxane: alternative materials for fabrication of organ-on-a-chip devices and microphysiological systems, ACS Biomater. Sci. Eng., 2020, 7, 2880–2899.
- 188 J. Nie, J. Fu and Y. He, Hydrogels: the next generation body materials for microfluidic chips?, *Small*, 2020, **16**, 2003797.
- 189 Q. Zhao, H. Cui, Y. Wang and X. Du, Microfluidic platforms toward rational material fabrication for biomedical applications, *Small*, 2020, **16**, 1903798.
- 190 S. Brittman, S. Z. Oener, K. Guo, H. Āboliņš, A. F. Koenderink and E. C. Garnett, Controlling crystallization to imprint nanophotonic structures into halide perovskites using soft lithography, *J. Mater. Chem. C*, 2017, 5, 8301–8307.

- 191 W. Wang, Y. Q. Liu, Y. Liu, B. Han, H. Wang, D. D. Han, J. N. Wang, Y. L. Zhang and H. B. Sun, Direct laser writing of superhydrophobic PDMS elastomers for controllable manipulation via Marangoni effect, *Adv. Funct. Mater.*, 2017, 27, 1702946.
- 192 W. Li, D. Kitagawa, S. Kobatake, E. Bekyarova and C. J. Bardeen, Patterning submicron photomechanical features into single diarylethene crystals using electron beam lithography, *Nanoscale Horiz.*, 2022, 7, 1065–1072.
- 193 D. Ebert and B. Bhushan, Transparent, superhydrophobic, and wear-resistant surfaces using deep reactive ion etching on PDMS substrates, *J. Colloid Interface Sci.*, 2016, **481**, 82–90.
- 194 G. Gonzalez, A. Chiappone, K. Dietliker, C. F. Pirri and I. Roppolo, Fabrication and Functionalization of 3D Printed Polydimethylsiloxane-Based Microfluidic Devices Obtained through Digital Light Processing, Adv. Mater. Technol., 2020, 5, 2000374.
- 195 M. Li, S. Li, J. Wu, W. Wen, W. Li and G. Alici, A simple and cost-effective method for fabrication of integrated electronic-microfluidic devices using a laser-patterned PDMS layer, *Microfluid. Nanofluid.*, 2012, **12**, 751–760.
- 196 S. J. Shepherd, C. C. Warzecha, S. Yadavali, R. El-Mayta, M.-G. Alameh, L. Wang, D. Weissman, J. M. Wilson, D. Issadore and M. J. Mitchell, Scalable mRNA and siRNA lipid nanoparticle production using a parallelized microfluidic device, *Nano Lett.*, 2021, 21, 5671–5680.
- 197 A. Giorello, A. Nicastro and C. L. A. Berli, Microfluidic Platforms for the Production of Nanoparticles at Flow Rates Larger Than One Liter Per Hour, *Adv. Mater. Technol.*, 2022, 7, 2101588.
- 198 M. Sheybanifard, L. P. B. Guerzoni, A. Omidinia-Anarkoli, L. De Laporte, J. Buyel, R. Besseling, M. Damen, A. Gerich, T. Lammers and J. M. Metselaar, Liposome manufacturing under continuous flow conditions: towards a fully integrated set-up with in-line control of critical quality attributes, *Lab Chip*, 2023, 23, 182–194.
- 199 C. Webb, S. Ip, N. V. Bathula, P. Popova, S. K. V. Soriano, H. H. Ly, B. Eryilmaz, V. A. Nguyen Huu, R. Broadhead and M. Rabel, Current status and future perspectives on MRNA drug manufacturing, *Mol. Pharm.*, 2022, 19, 1047– 1058.
- 200 J. W. Shreffler, J. E. Pullan, K. M. Dailey, S. Mallik and A. E. Brooks, Overcoming hurdles in nanoparticle clinical translation: The influence of experimental design and surface modification, *Int. J. Mol. Sci.*, 2019, 20, 6056.
- 201 F. Benfenati and G. Lanzani, Clinical translation of nanoparticles for neural stimulation, *Nat. Rev. Mater.*, 2021, 6, 1–4.
- 202 N. Kamaly, Z. Xiao, P. M. Valencia, A. F. Radovic-Moreno and O. C. Farokhzad, Targeted polymeric therapeutic nanoparticles: design, development and clinical translation, *Chem. Soc. Rev.*, 2012, 41, 2971–3010.
- 203 S. Damiati, U. B. Kompella, S. A. Damiati and R. Kodzius, Microfluidic devices for drug delivery systems and drug screening, *Genes*, 2018, 9, 103.

Analyst Critical Review

- 204 K. Duval, H. Grover, L.-H. Han, Y. Mou, A. F. Pegoraro, J. Fredberg and Z. Chen, Modeling physiological events in 2D vs. 3D cell culture, Physiology, 2017, 32, 266-277.
- 205 M. Ravi, V. Paramesh, S. R. Kaviya, E. Anuradha and F. D. P. Solomon, 3D cell culture systems: advantages and applications, J. Cell. Physiol., 2015, 230, 16-26.
- 206 A. Ozcelikkale, H. r. Moon, M. Linnes and B. Han, In vitro microfluidic models of tumor microenvironment to screen transport of drugs and nanoparticles, Wiley Interdiscip. Rev.: Nanomed. Nanobiotechnol., 2017, 9, e1460.
- 207 A. Ozcelikkale, K. Shin, V. Noe-Kim, B. D. Elzey, Z. Dong, J.-T. Zhang, K. Kim, I. C. Kwon, K. Park and B. Han,

- Differential response to doxorubicin in breast cancer subtypes simulated by a microfluidic tumor model, J. Controlled Release, 2017, 266, 129-139.
- 208 H.-r. Moon, A. Ozcelikkale, Y. Yang, B. D. Elzey, S. F. Konieczny and B. Han, An engineered pancreatic cancer model with intra-tumoral heterogeneity of driver mutations, Lab Chip, 2020, 20, 3720-3732.
- 209 B. Kwak, A. Ozcelikkale, C. S. Shin, K. Park and B. Han, Simulation of complex transport of nanoparticles around tumor-microenvironment-on-chip, J. Controlled Release, 2014, 194, 157-167.